https://doi.org/10.5194/se-2019-106
Preprint. Discussion started: 26 July 2019
© Author(s) 2019. CC BY 4.0 License.

Solid Earth
Discussions
Open Access
EGU

Magmatic sulphides in high-K calc-alkaline to shoshonitic and alkaline rocks

Ariadni Georgatou[1], Massimo Chiaradia[1]

[1]Department of Earth Sciences, University of Geneva, Rue des Maraichers 13, 1205 Geneva, Switzerland

Correspondence to: Ariadni Georgatou (ariadni.georgatou@unige.ch)

Abstract. We investigate in both mineralised and barren systems the occurrence and chemistry of magmatic sulphides and their chalcophile metal cargo behaviour during evolution of compositionally different magmas in diverse geodynamic settings. The investigated areas are: (a) the Miocene Konya magmatic province (hosting the Doganbey Cu-Mo and Inlice Au-epithermal deposits) (Post-Subduction) and (b) the Miocene Usak basin (Elmadag, Itecektepe and Beydagi volcanoes, the latter associated with the Kisladag Au porphyry) in Western Turkey (Post-Subduction). For comparison we also investigate (c) the barren Plio-Quaternary Kula volcanic field, west of Usak (Intraplate) and finally we discuss and compare all the above areas with the already studied (d) Quaternary Ecuadorian volcanic arc (host to the Miocene Llurimagua Cu-Mo and Cascabel Cu-Au porphyry deposits) (Subduction). The volcanism of the studied areas ~~displays a wide range of SiO_2 spanning~~ from basalts to andesites/dacites and from high K-calc-alkaline to shoshonitic series. Multiphase magmatic sulphides occur in different amounts in all investigated areas, and based on textural and compositional differences, they can be classified in different types, which crystallised at different times (early versus late saturation). A decrease in the sulphide Ni/Cu (proxy for mss-monosulphide solid solution/iss-intermediate solid solution) ratio is noted with magmatic evolution. ~~Starting with~~ an early stage, ~~saturating~~ Ni-richer/Cu-poorer sulphides hosted by early crystallising minerals e.g. olivine/pyroxene, ~~leading up to a~~ later stage, ~~producing~~ Cu-rich~~er~~ sulphides hosted by magnetite. The most common sulphide type resulting from ~~an~~ early saturating ~~stage~~ is composed of a Cu-poor/Ni-rich (pyrrhotite/mss) and one/two Cu-rich (cubanite, chalcopyrite/iss) phases making up 84 and 16 area % of the sulphide, respectively. Our results suggest that independently of the magma composition, geodynamic setting and whether or not the system has generated an ore deposit on the surface, sulphide saturation occurred in variable degrees in all studied areas and magmatic systems and is characterised by a similar initial metal content of the magmas. However not all studied areas present all sulphide types and the sulphide composition is dependent on the nature of the host mineral. In particular sulphides, ~~-~~resulting from the late stage, consisting of Cu-rich phases (chalcopyrite, bornite, digenite/iss) are hosted exclusively by magnetite and are found only in magmatic provinces associated with porphyry Cu (Konya and Ecuador) and porphyry Au (Beydagi) deposits.

1. Introduction

Historically petrographic and mineral chemistry studies of magmatic sulphides have been carried out on magmatic sulphides associated with orthomagmatic Ni-Cu-PGE mineralised systems (e.g., Barnes et al., 2017, Mungall and Brenan, 2014). Recent studies, however, highlight the growing interest of research towards magmatic sulphides in porphyry ore-associated magma (e.g. Halter et al., 2005, Brennecka, 2006, Zhang and Audétat, 2017) and in barren volcanic provinces (e.g., Nadeau et al., 2010, Park et al., 2015, Fulignati et al., 2018, Zelenski et al., 2017, Keith et al., 2017, Savelyev et al., 2018) in order to track processes affecting the fertility of these systems. In fact,

https://doi.org/10.5194/se-2019-106
Preprint. Discussion started: 26 July 2019
© Author(s) 2019. CC BY 4.0 License.

Solid Earth
Discussions
Open Access
EGU

it is still unclear how sulphide saturation affects the process of magmatic-hydrothermal ore formation. On one hand early sulphide saturation will strip off chalcophile and siderophile elements from the melt rendering the residual melt less fertile ~~and~~ on the other hand magmatic sulphide- and metal-rich cumulates may represent a temporary storage, which subsequently releases chalcophile metals to the magmatic hydrothermal system (e.g. Nadeau et al., 2010, Wilkinson, 2013, Fontboté et al., 2017).

Georgatou et al. (2018) described the occurrence, texture and composition of magmatic sulphides in relation to the whole rock chemistry of Quaternary Ecuadorian volcanic rocks. Sulphides were found in all rocks ranging in composition from basalts to dacites, occurring as polymineralic inclusions composed of Fe-rich/Cu-poor and Cu-rich phases. The inclusions, of variable size (mostly 1-30 μm) and shape (globular, ellipsoidal, angular and irregular), were hosted mostly by Fe-oxides (magnetite) and, to a lesser extent, by silicates (amphibole, pyroxene and plagioclase). The Quaternary Ecuadorian volcanism represents a typical example of high Sr/Y (Loucks 2014, Chiaradia and Caricchi, 2017) calc-alkaline magmas (with Si[illegible] 50-67 wt%) occurring in a subduction ~~geodynamic~~ setting potentially ~~related to~~ porphyry and epithermal deposits (e.g. Junin, Llurimagua Cu-Mo and Cascabel Cu-Au Tertiary-Scütt[illegible]al., 2012 porphyry deposits and El Corazon high sulphidation epithermal deposit).

Although the majority of porphyry Cu (± Au) deposits are formed in association with Andean [illegible] subduction-related magmas (e.g. Sillitoe, 1972, Cooke et al., 2005) there is a growing evidence that numerous porphyry deposits are also related to post-subduction magmatism (Richards, 2009). The porphyry deposits found in both these settings present similarities in terms of mineralisation and alteration styles but also some differences concerning petrogenesis and geochemistry of associated magmas (Shafiei et al., 2009, Richards, 2009, Hou et al., 2011). By comparing the occurrence and composition of magmatic sulphides found in volcanic rocks from different geodynamic settings (which may host porphyry and epithermal deposits, Fig.1), it is possible to trace the chalcophile element evolution in those magmas and investigate the role of magmatic sulphide saturation with respect to the fertility of the ore forming systems.

In order to investigate the magmatic sulphide occurrence in volcanic rocks characterised by post-subduction geodynamic setting, we focus our study on three volcanic areas located in Western Anatolia (Turkey), namely the Konya volcanic belt, the Usak Basin (Elmadag, Itecektepe and Beydagi volcanoes) and the Kula volcanic field (Fig.2). The investigated areas represent a suitable integration of and comparison to Ecuador's study for the following reasons: (i) the wide range of SiO2 content (43-70 wt%) and alkalinity (from calc-alkaline to shoshonitic and alkaline affinities) characterising the volcanic rocks, (ii) the occurrence of both Cu and Au-rich porphyry, and epithermal-type deposits (Doganbey Cu-porphyry and Inlice Au-epithermal in Konya and Kisladag Au-porphyry in Beydagi) temporally associated with magmatic rocks of these areas, and (iii) the inclusion of the intraplate mafic alkaline volcanic field of Kula which is not associated with any type of mineralisation.

Contrary to the majority of previous studies, here (i) we do not focus explicitly on transparent/semi-transparent sulphide host minerals, (ii) we do not work with mineral separates, and (iii) we investigate uncovered sulphides. These three factors allow us to include the study of opaque minerals (e.g. magnetite) as hosts of magmatic sulphides and maintain the textural relations not only between the sulphide, its host mineral and the surrounding minerals but also within the sulphide inclusion itself.

https://doi.org/10.5194/se-2019-106
Preprint. Discussion started: 26 July 2019
© Author(s) 2019. CC BY 4.0 License.

2. Geology, Magmatism and Mineralisation in Western Anatolia

The geodynamic regime in Western Anatolia has switched from a subduction setting during the Upper Cretaceous to a collisional setting in the Late Paleocene resulting in post-collisional extension in the Eocene (Delibaş et al., 2016, 2017; see figure 2-a for the general geodynamic setting). Several volcano (-plutonic) complexes of Mio-Pliocene age occur in NE-SW-trending extensional basins and are post-orogenic extensional in nature. They have been divided into three regions (Fig.2b,c); (i) the Konya region, for which both subduction (Doglioni et al., 2009; Innocenti et al., 2010) and post-subduction (Pe-piper et al., 2001; Dilek and Altunkaynak, 2007) geodynamic regimes have been suggested, is here taken to represent a transitional geodynamic regime (from subduction to post-subduction), (ii) the Usak-Güre Basin, including three volcanic centers (Elmadag, Itecektepe and Beydagi), corresponds to a post-subduction, locally extensional setting (Prelević et al., 2012, Ersoy et al., 2010), and (iii) the Kula volcanic field results from asthenospheric upwelling associated with extension in a post-subduction setting (Tokcaer et al., 2005, Alici et al., 2002).

2.1 Konya

The Konya volcanic belt (KVB) is located S-SW of the city of Konya (Fig.2b). It is composed of volcanic domes and ignimbrites of Mid-Miocene to Pliocene age (Keller et al., 1977, Temel 2001). The basement includes Permian metamorphic rocks, Triassic limestone and shales, Jurassic ophiolites, radiolarites and limestones, Cretaceous sandstones and quartzites (Temel et al., 1998). The erupted products are andesites to dacites with high-K calc-alkaline affinity. According to K/Ar ages obtained by Keller et al. (1997) a southwestern migration of magmatism is observed with time, starting with the oldest unit, the Sille volcanics (11.45 Ma – 11.9 Ma), located in the northeastern part of the Konya volcanic and ending with the Fasillar and Gevrekli domes, in the SW of the volcanic belt, which show Pliocene ages (3.75 Ma and 3.35 Ma respectively).

The Konya volcanic belt hosts the Miocene Au-epithermal high sulphidation deposit of Inlice (59.600oz @ 2.36 g/t Au, mining-atlas.com, 2015) located in the Erenkaya dome and the Miocene-Pliocene Doganbey Cu porphyry deposit (drilling of 273.90m @ 0.13g/t Au, Stratex International Plc, 2018), situated in the Karadag-Doganbey dome, both shown in figure 2b. Two other prospects (Karacaoren and the Oglakci) have been discovered by Stratex International in the KVB.

2.2. Usak-Güre basin

The Usak-Güre basin, situated 300 km west of the KVB, is composed of (i) the Menders Massif, including a metamorphic core composed of metagranites and gneiss (Proterozoic) overlain by Paleozoic schists and Mesozoic marbles and of (ii) the Upper Cretaceous Ophiolitic mélange of the Izmir-Ankara zone including unmetamorphosed ultramafic rocks, radiolarites and altered silicic rocks (Ercan et al., 1978, Cemen et al., 2006). Syn-extensional sedimentation and volcanism associated with the metamorphic complex of the Menders Massif are recorded in detail within the basin. From early to late Miocene the basin contains three sequences: the Hacibekir Group, the Inay Group and the Asartepe formation, represented by volcanic and metamorphic rocks (Cemen et al., 2006, Karaoglou et al., 2010). The Cenozoic volcanism in the Usak-Güre basin occurs in three NE-SW trending belts where the volcanic edifices are aligned. According to the ages obtained by Karaoglou et al. (2010) and Seyitoglu (1997) it appears that the volcanism migrated from north to south with time: (i) Elmadag

https://doi.org/10.5194/se-2019-106
Preprint. Discussion started: 26 July 2019
© Author(s) 2019. CC BY 4.0 License.

(17.29 Ma), (ii) Itecektepe (15.04 Ma) and (iii) Beydagi (12.15Ma) (see figure 2c). Volcanic products includes shoshonites, latites and rhyolitic lavas followed by dacitic and andesitic pyroclastic deposits. All three volcanoes are composed of dacitic ignimbrites formed by the collapse of their caldera and overlying lava flows.

Among all the volcanic complexes situated in the Usak-Güre basin only the Beydagi complex has been recognised as mineralised hosting the Kisladag Au-porphyry (Baker et al., 2016, 457 Moz @ 0.61 g/t of total measured and indicated resources with Au cut-off grade 0.3 g/t, www.eldoradogold.com-last update on 30.9.18 and up to 327 ppm of Mo, Sillitoe, 2002).

2.3 Kula volcanic field

The Kula volcanic field is situated west of the Usak province (Fig.2c) and its volcanic products are late Pliocene to late Quaternary in age (Ercan and Oztunali, 1983; Ercan et al., 1983, Richardson, 1996, Innocenti et al., 2005, Aldanmaz, 2002, Westaway et al., 2004). The rocks include lava flows and tephra deposits of varying mafic alkaline composition (basanite, phonolitic tephrite and trachybasalt). Kula represents an intraplate OIB-like alkali-basaltic volcanic center with an asthenospheric mantle signature and no subduction-related inputs (e.g. Agostini et al., 2007, Alici et al., 2002, Tokcaer et al., 2005).

3. Analytical Methods

After ~~realising~~ a preliminary screening for magmatic sulphides in 108 thin sections from all investigated volcanic centres, a total number of 93 thin polished sections were studied in detail under a petrographic microscope both in transmitted and reflected light (Table S1 in Supplementary 1). Thin sections that had both hydrothermal and magmatic sulphides were excluded from this study due to the difficulty in some cases to distinguish between these two types of sulphides. For this reason, unless stated otherwise, sulphides referred to herein are always meant to be magmatic sulphides. Microphotographs and identification of mineral phases were obtained using a Scanning Electron Microscope (SEM) JEOL JSM7001F digital with 15kV accelerating potential and 1 nA absorbed current, at the University of Geneva, Switzerland. Whole-rock samples were analysed for major and minor elements by X-ray fluorescence analysis (XRF) using a PANalytical AxiosmAX spectrometer and for trace elements by a Laser Ablation Inductively Coupled Mass Spectrometer (LA-ICPMS Agilent 7700), at the University of Lausanne, Switzerland (Tables 1-3 in doi:10.6084/m9.figshare.8230787). In situ chemical analysis of sulphides (Table 1) was carried out using a JEOL 8200 ~~Electro~~ Probe Micro-Analyser (EPMA) at the University of Geneva, Switzerland (for complete dataset see Table 4 in doi:10.6084/m9.figshare.8230787). ~~An~~ image analysis software~~,~~ (ImageJ©1.38 software)~~,~~ was used to obtain modal abundances of the phases composing each sulphide in order to reconstruct the bulk (area %) sulphide composition (for complete dataset see Table 5 in doi:10.6084/m9.figshare.8230787). For details on analytical methods on whole rock and mineral chemistry see Supplementary 2.

https://doi.org/10.5194/se-2019-106
Preprint. Discussion started: 26 July 2019
© Author(s) 2019. CC BY 4.0 License.

4. Results

4.1. Whole rock geochemistry

The volcanism of the studied areas displays a wide range of SiO2 and alkali element concentrations ranging from basalts to andesites/dacites and from high K-calc-alkaline to shoshonitic series (Fig.3a,b). The KVB is characterised by volcanic products with a high K-calc-alkaline affinity ranging from andesitic to dacitic in composition. In the Usak basin, the Elmadag volcanic complex is composed mostly of shoshonitic trachyandesites, the Itecektepe volcanic unit is characterised by high K-calc-alkaline rocks, mostly andesitic in composition, and the Beydagi volcanic edifice contains high K-calc-alkaline to shoshonitic rocks ranging from andesites to trachyandesites. Finally the Kula Quaternary volcano presents the most alkaline and mafic compositions, ranging from tephrites/basanites to phonotephrites. All rocks present a negative correlation between TiO_2/Fe_2O_3 and SiO_2, with Kula being more enriched in TiO_2 and Fe_2O_3 than the rest.

In terms of trace element concentrations all rocks show a decrease of Cu and Ni with increase of SiO_2 (Fig.3e-f), indicating a compatible behaviour of these elements during magmatic evolution. In addition all rocks show an enrichment of LREE relative to HREE with decreasing Nb, Ta, [illegible] and Ni passing from intraplate volcanism (Kula) to post-subduction (Elmadag, Itecektepe, Beydagi) and finally to a transitional subduction to post-subduction regime (Konya).

4.2. Sample petrography

All studied samples are volcanic rocks with porphyritic textures. Phenocrysts are usually plagioclase, amphibole, pyroxene (mostly clinopyroxene) and, depending on the volcanic centre, olivine, biotite and to a lesser extent Fe-Ti oxides (mostly Ti-magnetite). The matrix is aphanitic, mostly composed of microlitic plagioclase (<1 mm) and sometimes amphibole and pyroxene microcrystals. Apatite and anhydrite can also be found as inclusions in pyroxene and Fe-Ti oxide phenocrysts.

4.3. Sulphide petrography and chemistry

Rocks of all study areas contain magmatic sulphides, however, depending on the volcanic centre, sulphides are present in variable amounts, size, shape and composition. A comparison of the sulphide occurrence between the different volcanic centers (corresponding also to different geodynamic settings) is given in figure 4. In all studied samples sulphides occur inside phenocrysts and not in the groundmass (Fig.5), with the exception of the Kula volcano that presents sulphides also as aggregates with oxides and micro-sized silicates in the groundmass (Figs.4e,ii,5e) and a few cases in Beydagi (Fig.4xi). The main host phenocryst for sulphides is magnetite for Konya and Beydagi (42% and 31% respectively), amphibole for Itecektepe and Kula (85% and 39%), and pyroxene for Elmadag (87%). Sulphides are also hosted in plagioclase (Fig.5b). Noteworthy is the frequent occurrence of voids/bubbles in contact with the sulphide phases (e.g. figs. 4ii, 5g).

Based on petrographic observations and SEM mineral analysis we distinguished six main types of magmatic sulphides: 1) sulphides containing two to three distinct phases, namely a Cu-poor and Ni-rich phase (pyrrhotite), a Ni-rich phase (pentlandite), and rarely a Cu-rich phase (cubanite) (Fig.4a); 2) two to four distinct phases, namely a Cu-poor (pyrrhotite), one/two Cu-rich (chalcopyrite ± cubanite) and sometimes a Ni-rich (pentlandite) phase (Fig.4b); 3) a Cu-rich phase (chalcopyrite or chalcocite) and an Fe-rich phase (pyrite) (Fig.4c); 4) only Cu-rich

https://doi.org/10.5194/se-2019-106
Preprint. Discussion started: 26 July 2019
© Author(s) 2019. CC BY 4.0 License.

phase/s (chalcopyrite, ± cubanite, ± bornite), occasionally in contact with anhydrite (Fig.4d); and 5) aggregates of a Cu-poor and Ni-rich (pyrrhotite) sulphide phase and one or more Al-rich oxide phases (magnetite, magnetite/ilmenite and secondary goethite) (Fig.4e). Finally type-6 sulphides, the so-called "daughter sulphides" (e.g., Savelyev et al., 2018, Fig.5h), were only observed in three cases in this study, within olivine phenocrysts of rocks from Kula. From SEM analysis this latter sulphide type it is composed only out of pyrrhotite ± pentlandite, however due to their small size (<0.5 μm) they were not analysed with the EPMA.

Type-1 sulphides are only hosted by olivine, they are generally small (<30 μm), round and show pn exsolution flames in po (Fig.4i). Type-2 sulphides, the most common, are hosted by different phenocrysts (pyroxene, amphibole, magnetite and plagioclase), presenting a range of sizes (up to 70 μm) and having mostly ellipsoidal to rounded shape (Fig.4ii-vii). The pentlandite phase in this sulphide type can occur either as an ~~exsolution~~ in the pyrrhotite and/or as an individual phase inside the Ni-rich pyrrhotite (Fig.4vi), whereas cubanite is mostly present when the sulphide is hosted in amphibole, forming complex exsolution textures with chalcopyrite and presenting irregular rounded-resorbed shapes (Fig.5d). Types- 3 and 4 sulphides are only hosted by magnetite phenocrysts occurring in smaller sizes (<30 μm and <20 μm) and presenting ellipsoidal and angular shapes, respectively (Fig.4viii,ix,x). Type-4 sulphides in particular have been observed in some cases in contact with anhydrite and with zircon inclusions (usually <20 μm) and altogether hosted by the same magnetite crystal (Fig.6). Finally type-5 consists of sulphide aggregates with variable size (up to 600 μm), which may carry rounded oxide inclusions and sometimes are in sharp contact with surrounding silicate phases (Figs.4xi,xii,5e). Although all study areas present type-2 sulphides, from the volcanic centers situated in the Usak basin, only Beydagi shows sulphide types-3 and 5, whereas only Kula and Konya present sulphide types 1 and 4, respectively.

Electron microprobe analysis confirms the above petrographic observations and SEM analysis. Sulphides belonging to Konya and to the volcanic areas of the Usak-Güre basin (Beydagi, Elmadag and Itecektepe) have compositions typical of the Cu-Fe-S system whereas sulphides observed in Kula (intraplate OIB-like volcanism) extend into the Cu-Fe-Ni system as well (Fig.7a,b). Sulphides from all areas present a range of compositions between pyrrhotite and cubanite-chalcopyrite (type-2,5) hosted by different phenocrysts (mostly amphibole, pyroxene and magnetite, Fig.7a). Beydagi shows additional compositions between chalcopyrite (sometimes chalcocite) and close or equal to magmatic pyrite (type-3) and Konya presents sulphides ranging from chalcopyrite to bornite compositions (type-4). The latter types are only hosted by magnetite. In the case of Kula a number of sulphides (type 1 and some type-2) are Ni-rich, ranging from pyrrhotite to pentlandite (Fig.7b). A general decrease in the sulphide Ni/Cu ratio versus Fe/S ratio can be noted switching from Ni-rich sulphide phases (pn) hosted by olivine to Cu-rich (bn) hosted by magnetite (Fig.7c).

~~Note that often~~ the ~~resulting~~ EPMA sulphide composition corresponds to variable nonstoichiometric atomic ratios of major components different from the typical expected base metal composition of the sulphide phase observed, resulting into intermediate values characteristic of a solid solution mostly between two end members (e.g. cb and cp, cp and bn Figs.6,7). In addition in some cases sulphides are characterised by a sulphur deficiency, which, according to previous studies, may be a result of the replacement of sulphur by oxygen that is not directly measured by EPMA (e.g. Larocque et al., 2000, Keith et al., 1997). These latter cases show usually lower totals than those resulting from Cu-rich type-4 sulphide analysis (see Table 4 in doi:10.6084/m9.figshare.8230787).

https://doi.org/10.5194/se-2019-106
Preprint. Discussion started: 26 July 2019
© Author(s) 2019. CC BY 4.0 License.

A sulphide comparison for each area in terms of Cu and Ni contents, determined by EPMA, is shown in figure 8. Konya presents the ~~Cu-richest~~ sulphides (type-4, Cu median= 56 wt %) and Kula the most Ni-rich sulphides (type-1, Ni median = 4.2 wt %). In the Usak basin Beydagi shows the ~~Cu-richest~~ sulphides (type-3, Cu median= 32 wt %), followed by Elmadag (type-2, Cu median= 0.14 wt %) and then by Itecektepe (type-2, Cu median= 0.03 wt %). In addition to Cu, Fe, Ni and S, sulphides were also analysed for As, Se, Zn, Ag and Au (see table C.1 for determination limits.). For all locations As and Se are generally lower than 0.1 wt %. Zn concentrations were obtained only for Konya and Kula, showing for type-2 sulphides, Zn median= 0.03 and 0.04 wt%, respectively. Out of 503 Ag and 196 Au sulphide measurements obtained, only 82 and 31 values, respectively, resulted in concentrations above detection/determination limit. Ag varies between 0.01-0.07 wt % with a maximum amount of 0.11 wt% (in Konya) whereas Au is higher showing higher values in the Usak-Güre basin (Au median=0.14-0.24 wt %) compared to the rest (Au median=0.04-0.05 wt %). These unusually high sporadic values of Ag and Au have been attributed by previous studies to clustering and nugget effects of noble metals (e.g. Savelyev et al., 2018, Zelenski et al., 2017, Holwell et al., 2015, Holwell and McDonald, 2010). A possible Au nugget occurrence is shown in figure 4viii for type-3 sulphides of Beydagi. Although the phase is too small (<0.5 μm) to obtain quantitative values by EPMA, detectable Au was measured by SEM near and on this high reflectance micro-phase.

Since all sulphide types are composed of more than one mineral phase and therefore a single sulphide may correspond to more than one EPMA value, the sulphide composition data has been presented here in two different ways: (a) as individual microprobe measurements for each sulphide type observed in the different study areas (Table 1, Figs.7,8) and (b) as reconstructed bulk compositions of the sulphide inclusion by considering the modal abundance (area %) and the EPMA concentrations for each phase composing the sulphide (Table 2, Figs. 9,10).

Calculating the area % in plan view of each mineral composing the sulphide (and therefore the mss/iss initial proportions) allows us to get an indirect information on the initial metal budget of the silicate melt from which the sulphide melt was exsolved in the different study areas. One could question that this approach may yield biased results (because of cut effects and crystal orientation), but averaged out over a large number of sulphides we think we obtain a significant first-order estimate. The mean proportions of mss and iss in area% are shown with the box plot of figure 9 and in table 2. The mss area % (=mss/(mss+iss)*100) and the 2 standard error for each study area are as follows: Kula (82.0±7.4 %), Itecektepe (84.8±4.9 %), Elmadag (86.9±4.8 %), Beydagi (86.9±3.2 %), Konya (88.1±2.6 %). A reconstruction of the bulk mss and iss in area (%) composition of the sulphides was realised in this study also for the case of Ecuador for comparative purposes, resulting in mss area% of 82.0±4.8. When considered all together (type-2 sulphides from all investigated areas), for a total of 100 sulphides, all study areas present similar proportions of Fe-rich/mss (84.2%) and Cu-rich/iss (15.7%) phases within error (2se = ± 2.2).

5. Discussion

5.1. Sulphide melt evolution

The evolution of sulphide melt has been studied through experiments considering the sulphide globules as closed systems that differentiate with decreasing T (e.g. Kullerud et al., 1969, Calibri, 1973, Naldrett and Gasparrini, 1971, Cabri, 1973, Craig and Scott, 1974, Tsujimura and Kitakaze, 2004, Holwell and McDonald, 2010, Naldrett,

https://doi.org/10.5194/se-2019-106
Preprint. Discussion started: 26 July 2019
© Author(s) 2019. CC BY 4.0 License.

2013 and references therein). Nonetheless there is a difficulty to correlate the different phase stability fields for the complete range of temperatures, i.e., 1200-100°C. This is due to the fact that the Fe-Ni-Cu-S system is a complex system characterised by a number of solid solutions and unquenched phases. In addition, the mineral assemblage composing the sulphides depends, among other factors (fO2 and fS2), on the initial metal budget of the silicate melt, and therefore on the metal contents of the exsolving sulphide melt, as well as on the P and T conditions under which this melt solidifies. A compilation of isothermal sections of the Cu-Fe-S system resulting from a number of experimental studies realised at different temperatures is presented in figure 10. For this study it is important to note at which approximate temperature intervals mineral phases can coexist and therefore a summary of the experimental findings, only focused on the mineral phases observed in this study, has been added below.

The general agreement is that above 1200°C the system is composed of two immiscible liquids, a metal (Cu, Au)-rich liquid and a sulphur (+Fe, Ni)-rich liquid (Craig and Kullerud, 1969). An Fe, Ni-rich/Cu-poor monosulphide solid solution (mss) and a Cu, Au-rich/Ni-poor intermediate solid solution (iss) exsolve around 1192°C (Jensen, 1942) and 960°C (Kullerud et al., 1969), respectively (Fig.10a-b and 10c). The pair mss-iss is stable only starting from 935°C and until 590°C (Fig.10c-e), below which temperature these two phases cannot coexist. Around 930°C a high temperature-bornite solid solution (bnss-h) and iss become stable (Fig.10c). With further cooling (~610°C, Fig.10e) the mss converts to pyrrhotite (po), through exsolution of a high temperature pentlandite (pn-h) (e.g. Stone et al., 1989). Subsequently at 590°C the iss unmixes into chalcopyrite (cp) and cubanite (cb) (Fig.10f) (e.g. Yund and Kullerud, 1966). Pyrite (py) appears at 743°C and becomes stable with iss at 739°C and with cp at 600°C (Fig.10e). The pair cp-py coexists until at least 200°C (Craig and Scott, 1974). A low temperature pentlandite (pn) appears at 610°C and becomes stable with cp at 572°C. Finally the bnss-h breaks down to chalcocite (cc) and digenite (dg)-bnss pair at 430°C (Fig.10g). At 334°C po becomes stable with cp and with further cooling at 330°C the dg-bnss pair breaks down to dg and bornite (bn) (Fig.10g-h).

Two are the main stages of sulphide evolution observed in this study confirming the experimental temperature range windows, for specific mineral pairs, as well as previous research by Hattori, 1999, Parat et al., 2011, Du et al., 2014, Agangi et al., 2016. The first stage accounts for the more primitive sulphide types (1 and 2) including mss-rich±iss and mss + iss sulphide melt, now represented by compositions close to pyrrhotite (±pn, cb) and pyrrhotite + chalcopyrite (±cb), respectively. Their shape (round-ellipsoidal) and host mineral (olivine, amphibole, pyroxene, plagioclase and magnetite) confirm their origin as Fe-Ni (±Cu) - rich sulphide melts. The second stage consists of sulphide type 4, characterised by iss-only, sulphide liquid rich in Cu (since all Ni has been exhausted), now consisting of chalcopyrite and bornite (±dg). This sulphide type occurs only within Fe-oxides, mostly in Ti-rich magnetite with occasional ilmenite exsolution lamellae. Their angular shape indicates that the solution was trapped initially as a Cu-rich liquid (Chang and Audétat, 2018) which solidified into an iss following the host mineral crystallisation planes and later unmixed (see also Georgatou et al., 2018, Holwell et al., 2015). In addition to the relatively low temperature ranges compared to the first stage sulphides (<330°C, see Fig.10), other petrographic and compositional arguments for considering this ~~latter stage~~ as a later stage are the following: (i) the unique occurrence in magnetite, a late crystallising mineral relative to olivine and pyroxene (hosting the first stage sulphide types-1 and 2) and (ii) the more ~~dominant~~ occurrence of voids around the Cu-rich sulphides

https://doi.org/10.5194/se-2019-106
Preprint. Discussion started: 26 July 2019
© Author(s) 2019. CC BY 4.0 License.

accounting for higher mean portions of the inclusions (up to 23 area %, see tables 2,C.2) compared to type-2 sulphides (<10 area%). These voids could account for the presence of a pre-existing fluid phase (table 2).

Sulphide types-3 and 5 are more difficult to interpret. Type-3 presents both ellipsoidal and rectangular shapes indicating entrapment as a liquid/melt. The T range that corresponds to the mineral assemblage of chalcopyrite (±cc) + pyrite is 600-200°C, suggesting a later timing than the first stage sulphides. Finally type-5 sulphide aggregates are similar to the first stage sulphides (type 2) and seem to have originated from an mss and Fe-rich system, producing immiscibility textures of the rounded oxide inclusions into the pyrrhotite, which have later aggregated with silicates.

In this study we have not observed even one single case where early and late sulphides are co-hosted by the same mineral. This suggests two distinct saturating stages, ~~for which~~ in order to ~~rich~~ the second stage the system has to undergo ~~first~~ magnetite crystallisation. However, it is still not clear whether these stages are indeed distinct and independent one to another, or if they may follow '~~shortly~~' one another, through a continuous process of sulphide saturation, whose products change chemistry due to the chemical evolution of the melt. Nonetheless, according to the sulphide types observed in these two stages, the Ni/Cu (proxy for mss/iss) decreases with magmatic evolution (Fig.7c), starting from an mss-rich sulphide melt (type-1), followed by an mss and iss-melt (type-2,5) and finally (and uniquely for some settings) by iss-rich/only sulphides (type-3,4). Although this decrease in Ni/Cu has been noted previously by other researchers (e.g. Hattori, 1999, Du et al., 2014, Keith et al., 2017, Savelyev et al., 2018) for the early sulphides, until now, there has not been a systematic study on the later stage, iss-only sulphides. The reason for this is most likely the fact that the majority of past studies on sulphides have focussed on silicate mineral separates, in order to be able to locate and analyse the bulk chemistry of entrapped sulphides. This not only prevents necessary observations on textural mineral relations but also the study of non-transparent/opaque minerals, which, as it was shown here, host the iss-only/~~Cu-richest~~ sulphides.

5.2. Sulphide comparison in Western Anatolia

Volcanic rocks from all study areas contain sulphides and therefore have reached magmatic sulphide saturation at some stage during the lifespan of the magmatic system; however, there are significant textural and compositional differences, which are described below.

5.2.1. Kula volcanic field

In Kula we observe sulphide types (1, 2 and 5) representing the most primary Ni-rich and Cu-poor magmatic products resulting from an initial mostly mss-rich sulphide melt exsolving from a silicate melt. These sulphide types are similar to those found in MORBs (e.g. Patten et al., 2012, Keith et al., 2017, Savelyev et al., 2018 and references therein) and represent only a first stage sulphide saturation. From textural evidence, e.g., decompression rims in amphibole (Fig.5c), complex textures of cubanite-chalcopyrite resulting from rapid unmixing of iss due to T drop (Fig.5d, type-3) as well as the intact sulphide aggregates found in the groundmass (figure 5e, type 6), the magma in Kula seems to have ascended ~~fast~~ from depth (e.g. Tokcaer et al., 2005). This implies a short residence time in the crust, which in turns explains the minimum crustal contamination (e.g. Dilek and Altunkaynak, 2007, Alici et al., 2002) and the mafic rock composition.

https://doi.org/10.5194/se-2019-106
Preprint. Discussion started: 26 July 2019
© Author(s) 2019. CC BY 4.0 License.

5.2.2. Konya

For the case of Konya, the sulphide types found (2 and 4) represent both stages of sulphide saturation and are less primitive than the ones seen in Kula, with little or no pn present and always a Cu-rich phase (cp±bn). This suggests that the mss and iss-rich sulphide melt started exsolving from the silicate melt at a later stage of magmatic evolution, when the melt was already depleted in Ni and had already a higher amount of iss available, compared to Kula. In fact, the type 4 iss-only sulphide melt (representing the second/later stage sulphide saturation) of Konya has ~~sequestrated~~ Cu more successfully than at any other location investigated.

Konya is the unique example in this study presenting anhydrite inclusions in contact with a sulphide phase or hosted by the same magnetite phenocryst as the sulphide inclusion (Fig.6). The occurrence of anhydrite either in contact or along with Cu-rich sulphide phases, has been mentioned in the past (e.g., Hattori, 1993, Audétat and Pettke, 2006) and has been suggested to indicate a rapid drop of fO_2 of the system from the sulphate (>NNO+1) to the sulphide stability field (<NNO) allowing the magma to contain both reduced and oxidized forms of sulphur (Wilke et al., 2011). From experimental constraints for a water saturated system at 150-400 MPa and 1 wt% S added, anhydrite can coexist with pyrrhotite for fO2 = NNO+1 at 700°C, for fO_2 = NNO+1.5 at 800°C and for fO_2 = NNO+2.5 at 950°C (Parat et al. 2011 and references therein). Therefore, the occasional occurrence of anhydrite in this second stage sulphides (type-4), would indicate higher temperatures. However, in this study the sulphide mineral phases with which anhydrite coexists are Cu-richer/S-poorer (cp+bn±dg) than pyrrhotite, and are stable at higher fO_2 conditions and lower T. In addition, the system is not expected to be already water saturated and therefore the temperature ranges in which anhydrite will be stable can differ.

5.2.3. Usak-Güre Basin

Beydagi shows slightly more enriched (though similar within error) Cu values in type-2 sulphide (Cu median= 0.3 wt %) than Elmadag (Cu median= 0.14 wt %) and Itecektepe (Cu median= 0.03 wt %). Additionally, the area (%) of the Cu-phases/iss of type-2 sulphides found in Elmadag (17.2±4.8), Itecektepe (14.7±4.9) and Beydagi (13.1±3.2) is similar. However, Beydagi is the only volcanic center within the Usak basin which is characterised by two other sulphide types (3 and 5), and at the same is the only mineralised volcanic center. Implications regarding the ore fertility of these systems will be discussed in the following section. Relative to the other investigated areas of Western Anatolia, sulphides in Beydagi show no pentlandite but present in some cases chalcopyrite (±cc) coexisting with pyrite, suggesting that the iss-rich exsolving sulphide melt was Cu-rich~~er~~ relative to Kula but Cu-depleted relative to Konya.

5.3. Comparison with Ecuador

Various Miocene large Cu-Mo±Au porphyry deposits (e.g., Junin/Llurimagua Cu–Mo deposit and the Cascabel Cu–Au rich deposit) occur in the frontal arc of Ecuador. Available data on whole rocks indicate that mineralisation is spatially and temporally associated with high Sr/Y porphyritic stocks (Schütte et al., 2012). Investigation of these rocks under a reflected petrographic microscope confirmed previous observations from Schütte et al. (2012) that the rocks contain abundant hydrothermal sulphides, rendering these samples inadequate for the scope of the present study. For this reason, Georgatou et al. (2018) have investigated fresh volcanic rocks from the Quaternary arc of Ecuador. These are calc-alkaline magmatic rocks with high Sr/Y values erupted through a crust with a

https://doi.org/10.5194/se-2019-106
Preprint. Discussion started: 26 July 2019
© Author(s) 2019. CC BY 4.0 License.

thickness ranging from 50 to 70 km (Feininger and Seguin, 1983, Guillier et al., 2001). Such features are similar to those of magmatic systems typically associated with large porphyry Cu deposits (Loucks, 2014, Chiaradia and Caricchi, 2017) and the temporal and spatial proximity of Miocene deposits to the Quaternary arc rocks investigated lend support to the possibility that processes leading to the formation of porphyry type deposits under the Quaternary arc of Ecuador could be currently ongoing. Therefore, the Quaternary arc rocks of Ecuador can be used as a proxy of a potentially fertile typical Andean subduction-related magmatic environment.

In the barren Quaternary volcanics Georgatou et al. (2018) observed that magmatic sulphides occurred in all studied rocks (from basalt to dacite) of the volcanic arc as polymineralic inclusions composed of Fe-rich/Cu-poor and/or Cu-rich phases, occurring mostly in Fe/Ti oxides and to a lesser extent in silicate minerals. Only sulphide types-2 and 4 were observed in Ecuador, presenting ~~thus~~ a remarkable textural and compositional resemblance to the case of Konya. Both areas are characterised from both, first and second stage sulphide saturation. Nonetheless type-4 sulphides in Konya have ~~sequestrated~~ higher amounts of Cu compared to Ecuador, Cumax = 72 and 66 wt % respectively.

Georgatou et al. (2018) suggested that the negative trend of Cu with magmatic differentiation (e.g., Keith et al., 1997, Chiaradia, 2014) observed in typical Andean-type magmatic arcs is a result of a continuous Cu sequestration in magmatic sulphides. A similar Cu decrease with magmatic evolution is observed also in the areas studied here and characterised by post-subduction magmatic rocks some of which are also associated with porphyry and epithermal-type deposits. This suggests that in both settings (subduction and post-subduction) Cu and other chalcophile metals behave compatibly during magmatic evolution and confirms that these metals are lost on the way to the surface ~~within the continental crust~~.

In contrast to ~~the case of~~ Ecuador, the volcanic provinces of Konya and Beydagi are associated with coeval economic deposits. In particular, the Beydagi volcanic center was active from ~16 to 12 Ma and hosts the ~14 Ma Kisladag Au-porphyry, whereas the Konya Volcanic Belt is characterised by more or less continuous magmatism between ~12 and 3.3 Ma and hosts the ~7.2 Ma old (Zürcher et al., 2015) Doganbey Cu-porphyry and the Miocene (Redwood, 2006, Hall et al., 2007) Inlice Au-epithermal deposit.

6. Implications for ore formation

Konya, Beydagi (Usak basin) and Ecuador are the only areas among those studied, ~~which~~ are associated or potentially associated with economic deposits of the porphyry suite. It is remarkable that this feature coincides with the fact that rocks from these areas are the only ones with iss-only (type 4) and iss-richer (type-3) sulphides. In particular, type 4 sulphides (cp-bn±dg) were observed in areas associated (Konya) or potentially associated (Ecuador) porphyry Cu deposits (e.g. Konya-Doganbey and Ecuador-Cascabel/Llurimagua-Junin). Beydagi, where type 3 sulphides (cp-py) are seen, is associated with a porphyry Au deposit (Kisladag). The above observation calls for further investigation since the presence of iss-rich and iss-only sulphide types, like in cases 3 and 4, could be used as a proxy for porphyry-Cu and porphyry-Au type deposits, respectively.

Some of the most discussed contributing factors to the fertility of a magmatic system and its potential to produce a porphyry deposit on the surface, involve source fertility, in terms of initial CSE concentration and water amount, and later enrichment of the system in chalcophile elements by pre-concentration of CSEs in sulphide-rich zones.

https://doi.org/10.5194/se-2019-106
Preprint. Discussion started: 26 July 2019
© Author(s) 2019. CC BY 4.0 License.

For source fertility to play an important role for the ore genesis in terms of metal budget, it would imply an obvious difference in the Cu amount of the sulphides saturating during the first stage as well as different proportions of mss and iss composing the most primitive sulphides (type 2) for the different study areas. This would be a result of different metal abundances in the initial silicate melt that would preferentially partition into either the iss (eg. Cu, Au) or the mss (eg. Ni, Fe), respectively. However, there are no significant differences in the Cu values of type-2 sulphides nor in the mss/iss proportions among the areas that present iss-only sulphides and are associated with porphyry deposits. All study areas are characterised by similar Cu amount (Cu median= 0.03- 1.3 wt %) and proportions (area %) of Ni-rich/mss (84.2) and Cu-rich/iss (15.7) phases within uncertainty (2se = ± 2.2). These values are very similar to the mss-iss proportions characterising sulphides found in Merapi volcano (Nadeau et al., 2010), being mss= 81± 7 and iss= 19±7, respectively. This observation carries major implications suggesting that independently from the geodynamic setting (subduction, post-subduction and intraplate-OIB like volcanism) the initial metal abundances of the magma are approximately the same.

Concerning the water amount of the source, it is possible that different water content of the primitive magmas corresponding to different geodynamic settings may play an important role for both sulphide saturation at depth and ore generation at surface (e.g. Kelley and Cottrell, 2009, Richards, 2011, Yang et al., 2015). It is likely that all magmatic systems have the potential to become saturated in Cu-rich/iss-only sulphides, after exhausting all the Ni, as long as there is not enough water to strip out the metals from the melt, rendering a residual magma fertile, leading to the formation of a porphyry deposit. Based on the textural and chemical evidence from type 4 sulphides of Konya, here we may be able to trace the transition from a sulphide-saturated system to a fluid-saturated system. In addition, in this study, only areas that are characterised by a subduction component, and therefore by likely higher water contents in their source, resulted in Cu-rich sulphide saturation, with the counterexample of the intraplate OIB-like volcanism of Kula.

Sulphide pre-concentration in cumulates at depth and a later magmatic recycling through remelting and release of the metals back to the system seems a likely possibility (e.g. Audetat and Simon, 2012, Sillitoe, 2012, Wilkinson, 2013, Chiaradia, 2014, Jenner, 2017, Fontboté et al., 2017). Although we cannot test this hypothesis in the present study, it is possible that the sulphide-silicate-oxide aggregates observed in Kula (Figs.4xi, 5e) account for those cumulates. Further investigation of those types of cumulates through an experimental approach aiming to quantify the physico-chemical conditions under which this process may happen, would be needed.

An additional important factor in order to saturate sulphide Cu-rich phases is magnetite crystallisation. Although it has already been pointed out as an important step for sulphide saturation in general (e.g. Metrich et al., 2009, Jenner et al., 2010) in this study we show that magnetite crystallisation seems not necessary for any kind of sulphide saturation, but is systematically associated with the iss-rich (cp-py) and iss-only (cp-bn/dg), Cu-rich sulphide types (3 and 4). Only rocks that have undergone magnetite crystallisation present Cu-richer sulphides, with the exception of Kula as well as the cases of Elmadag and Itecektepe (Fig.7). These three volcanic centers are not associated with any known economic deposit.

We argue that the later sulphide types 3 and 4 (iss-rich/only, hosted in magnetite) can help us to further understand the transition between a sulphide-saturated system and a fluid-saturated system. In addition taking into consideration how porphyry deposits in subduction settings are generally Cu-rich whereas those found in post-

https://doi.org/10.5194/se-2019-106
Preprint. Discussion started: 26 July 2019
© Author(s) 2019. CC BY 4.0 License.

subduction settings tend to be Au-rich (e.g. Sillitoe, 1993, Li et al, 2006, Richards, 2009), future sulphide trace element LA-ICP-MS analysis including precise Au, Ag and PGE values (which constitute better markers for sulphide saturation identification, see Park et al., 2015, Cocker et al., 2015, Jenner, 2017, Mandon, 2017) will help distinguish the conditions of magma fertility for the different geodynamic settings. Finally magmatic sulphide saturation will retain a certain amount of CSEs and deplete the residual melt in them. Quantifying this metal loss is crucial in order to understand whether, for the bigger picture of ore forming processes, this loss is significant or not. Modelling combined with experimental results on metal partition coefficients, petrographic observations and data compilation of real case sulphide mineral analysis can aid to solve this question.

7. Conclusions

Four are the main conclusions of this study: (1) Sulphide saturation occurred in all study areas, independently of the magma composition, geodynamic regimes and whether or not the system produced an economic deposit. Sulphides were present in all rocks, corresponding to a wide range of composition (SiO_2 range = 46-68 wt.%, basalts to andesites/dacites and from high K-calc-alkaline to shoshonitic series), characterised by different geodynamic regimes (subduction, post-collision and intraplate OIB volcanism) some of which are associated with economic deposits (porphyry Cu and/or Au and Au epithermal); (2) According to their occurrence and chemical composition sulphides can be classified in different types and do not necessarily appear in all study areas. Type-1 sulphides are rare, mostly composed of Cu-poor phases (po, pn – mss), hosted only by olivine phenocrysts and are seen only in Kula. Type-2 sulphides consist of a Cu-poor phase (po, ±pn), and a Cu-richer phase (cb, cp). They are the most abundant type, hosted by different minerals (pyroxene, amphibole, magnetite, and plagioclase) and are found in all study areas. Type-3 sulphides are rare, composed of mostly a Cu-rich phase (cp±cc) and py, hosted by magnetite and are observed only in Beydagi. Type-4 sulphides are less abundant than type-2 but more abundant than types-1 and 3. They are composed of only Cu-rich phases (cp-bn±dg), hosted only by magnetite and observed solely in Konya and Ecuador. Type-5 sulphides are found in the groundmass as sulphide-oxide-silicate aggregates: they are mostly found in Kula and the sulphides are mainly Cu-poor. Types-3 and 4 are the sulphides with the highest Cu contents and are only observed in areas associated with porphyry Au and Cu deposits, respectively, together with epithermal Au deposits. (3) The initial metal content of the magma was very similar for all the study areas. This can be inferred from the similar proportions of the mss and iss of the early saturating stage sulphide (type-2) for all investigated study areas mss=84.2 and iss=15.7 area%, with 2se=± 2.2. Based on the points 2 and 3 above, the correlation between sulphides high in Cu and ore deposits, combined with the similar mss/iss proportions for all study areas suggests a later Cu-enrichment for the cases of Beydagi, Konya and Ecuador. (4) As the sulphide melt evolves, a decrease in Ni/Cu is observed, which is here used as a proxy for the mss/iss ratio. This chemical evolution corresponds to a sulphide melt evolution starting with an mss-rich sulphide melt, switching to an mss and iss-melt and finally (and uniquely for some settings) to iss-only sulphides. This suggests at least two sulphide saturating stages: an early mss-only or mss-richer and a late iss-only or iss-richer stage. Further research needs to address the question whether these stages are distinct or are part of a continuous process of sulphide saturation.

https://doi.org/10.5194/se-2019-106
Preprint. Discussion started: 26 July 2019
© Author(s) 2019. CC BY 4.0 License.

8. Author Contribution

AG and MC designed the project and methodology. AG carried out petrographical investigation, EPMA sulphide analysis and bulk rock chemical analysis. AG wrote the manuscript with contributions from MC.

9. Acknowledgements

This study is funded by the Swiss National Science Foundation (grant N. 200021_169032). We would like to acknowledge Luca Paolillo, Florian Franziskakis, Bastien Deriaz and Pablo Lormand for collecting samples from the Usak-Gure basin and from the Konya volcanic belt, during fieldwork in May 2016 as well as conducting part of the whole rock analysis, in the framework of their Master Thesis, supervised by Dr. Chiaradia Massimo at the University of Geneva.

10. References

Agangi, A., Reddy, S.M.: Open-system behaviour of magmatic fluid phase and transport of copper in arc magmas at Krakatau and Batur volcanoes, Indonesia. J. Volcanol. Geoth. Res., 327, 669–686, doi: 10.1016/j.jvolgeores.2016.10.006, 2016.

Agostini, S., Doglioni, C., Innocenti, F., Manetti, P., Tonarini, S., Savaşçin, M.Y.: The transition from subduction-related to intraplate Neogene magmatism in the Western Anatolia and Aegean area. Geol. S. Am. S., 418, 1-15, doi: 10.1130/2007.2418(01), 2007.

Aldanmaz, E.: Mantle source characteristics of alkali basalts and basanites in an extensional intracontinental plate setting, western Anatolia, Turkey: implications for multi-stage melting. Int. Geol. Rev., 44, 440–457, doi: 10.2747/0020-6814.44.5.440, 2002.

Alici, P., Temel, A., Gourgaud, A.: Pb–Nd–Sr isotope and trace element geochemistry of Quaternary extension-related alkaline volcanism: a case study of Kula region (Western Anatolia, Turkey). J. Volcanol. Geoth. Res., 115, 487-510, doi: 10.1016/S0377-0273(01)00328-6, 2002.

Audétat, A., Simon A.C.: Magmatic controls on porphyry copper genesis. In: Hedenquist J. W. Harris M. Camus F. (eds) Geology and Genesis of Major Copper Deposits and Districts of the World: A Tribute to Richard H. Sillitoe. Soc. Eco. Geo. Spc. Pub., 16, 553 – 572, 2012.

Audétat, A., Pettke, T.: Evolution of a Porphyry-Cu Mineralized Magma System at Santa Rita, New Mexico (USA). J. Petrol., 47, 2021-2046, doi: 10.5382/SP.16.21, 2006.

Baker, T., Bickford, D., Juras, S., Oztas, Y., Ross, K., Tukac, A., Rabayrol, F., Miskovic, A., Friedman, R., Creaser, A.R., Spikings, R.: The Geology of the Kisladag porphyry gold deposit, Turkey. Soc. Eco. Geo. Spc. Pub., 19, 57-83, doi: 10.5382/SP.19.03, 2016.

Barnes, S.J., Holwell, D.A., Le Vaillant, M.: Magmatic sulfide ore deposits. Elements, 13, 91–97, doi: 10.2113/gselements.13.2.89, 2017.

Brennecka, G.: Origin and metal content of magmatic sulfides in Cu-Au mineralizing silicic magmas: Yerington, Nevada and Yanacocha, Peru. M.S. thesis, Oregon State University, https://ir.library.oregonstate.edu/concern/graduate_thesis_or_dissertations/rn301373p, 2006.

Cabri, L.J.: New data on phase relations in the Cu-Fe-S system. Econ. Geol., 68, 443-454, doi: 10.2113/gsecongeo.68.4.443, 1973.

Çemen, I., Catlos, E.J., Gogus, O.H., Ozerdem, C.: Postcollisional extensional tectonics and exhumation of the Menderes massif in the Western Anatolia extended terrane, Turkey. Geol. S. Am. S., 409, 353-379, doi: 10.1130/2006.2409(18), 2006.

Chang, J., Audétat, A.: Petrogenesis and Metal Content of Hornblende- Rich Xenoliths from Two Laramide-age Magma Systems in Southwestern USA: Insights into the Metal Budget of Arc Magmas. J. Petrol., 59, 1869-1898, doi: 10.1093/petrology/egy083, 2018.

Chiaradia, M.: Copper enrichment in arc magmas controlled by overriding plate thickness. Nat. Geosci., 7, 43–46, doi: 10.1038/ngeo2028, 2014.

Chiaradia, M., Caricchi, L.: Stochastic modelling of deep magmatic controls on porphyry copper deposit endowment. Sci. Rep-UK., 7, 44523, doi: 10.1038/srep44523, 2017.

Cocker, H.A., Valente, D.L., Park, J.W., Campbell, I.H.: Using platinum group elements to identify sulfide saturation in a porphyry Cu system: the El Abra porphyry Cu deposit, Northern Chile. J. Petrol., 56, 2491-

https://doi.org/10.5194/se-2019-106
Preprint. Discussion started: 26 July 2019
© Author(s) 2019. CC BY 4.0 License.

2514, 2015.
Cooke, D.R., Hollings, P., Walsh, J.L.: Giant porphyry deposits: characteristics, distribution, and tectonic controls. Econ. Geol., 100, 801–818, doi: 10.1093/petrology/egv076, 2005.
Craig, J.R., Kullerud, G.: Phase relations in the Cu-Fe-Ni-S system and their application to magmatic ore deposits, doi: 10.5382/Mono.04, 1969.
Craig, J.R., Scott, S.D.: Sulfide phase equilibria. P.H. Ribbe (Ed.), Sulfide Mineralogy – Short Course Notes, 1, Mineralogical Society of America, Southern Printing Co., Blacksburg, Virginia, CS1–110, ISBN13 978-0-939950-01-0, 1974.
Delibaş, O., Moritz, R., Chiaradia, M., Selby, D., Ulianov A, , Revan, K.M.: Post-collisional magmatism and ore-forming systems in the Menderes massif: new constraints from the Miocene porphyry Mo–Cu Pınarbaşı system, Gediz–Kütahya, western Turkey. Miner. Deposita, 52, 1157-1178, doi: 10.1007/s00126-016-0711-7, 2017.
Delibaş, O., Moritz, R., Ulianov, A., Chiaradia, M., Saraç, C., Revan, K.M., Göç, D.: Cretaceous subduction-related magmatism and associated porphyry-type Cu–Mo prospects in the Eastern Pontides, Turkey: new constraints from geochronology and geochemistry. Lithos, 248, 119-137, doi: 10.1016/j.lithos.2016.01.020, 2016.
Dilek, Y., Imamverdiyev, N., Altunkaynak, S.: Geochemistry and tectonics of Cenozoic volcanism in the Lesser Caucasus (Azerbaijan) and the peri-Arabian region: collision-induced mantle dynamics and its magmatic fingerprint. International Geology Review, 52, 536-578, doi: 10.1080/00206810903360422, 2010.
Dilek, Y., Altunkaynak, Ş.: Cenozoic crustal evolution and mantle dynamics of post-collisional magmatism in western Anatolia. Int. Geol. Rev., 49, 431-453, doi: 10.2747/0020-6814.49.5.431, 2007.
Doglioni, C., Agostini, S., Crespi, M.., Innocenti, F., Manetti, P., Riguzzi, F., Savascin, Y.: On the extension in western Anatolia and the Aegean Sea. J. Virtual Explorer, 8, 169-183, doi: 10.3809/jvirtex.2002.00049, 2002.
Doglioni, C., Tonarini, S., Innocenti, F.: Mantle wedge asymmetries and geochemical signatures along W-and E–NE-directed subduction zones. Lithos, 113, 179-189, doi: 10.1016/j.lithos.2009.01.012, 2009.
Du, Y., Qin, X., Barnes, C., Cao Y., Dong, Q., Du, Yangsong, D.: Sulphide melt evolution in upper mantle to upper crust magmas Tongling, China. Geosci. Front., 5, 237-248, doi: 10.1016/j.gsf.2013.06.003, 2014.
Ercan, T., Satir, M., Kreuzer, H., Türkecan, A., Günay, E., Cevikbas, A., Ates, M., Can, B.: Batı Anadolu Senozoyik volkanitlerine ait yeni kimyasal, izotopik ve radyometrik verilerin yorumu. Turkiye Jeoloji Kurumu Bulteni, 28, 121-136, 1985.
Ercan, T., Dincel, A., Metin, S., Turkecan, A., Gunay, E.: Geology of the Neogene basins in the Usak region. Bull. Min. Res. Exploration. (in Turkish), 21, 97–106, 1978.
Ercan, T., Oztunali, O.: Characteristic features and "base surges" bed forms of Kula volcanics. Bull. Geol. Soc. Turkey. (in Turkish with English abs), 25, 117-125, 1982.
Ercan, T., Türkecan, A., Dinçel, A., Günay, A.: Geology of Kula-Selendi (Manisa) area. Geol. Engineering. (in Turkish), 17, 3–28, 1983.
Ersoy, E.Y., Helvacı, C., Palmer, M.R.: Mantle source characteristics and melting models for the early-middle Miocene mafic volcanism in Western Anatolia: implications for enrichment processes of mantle lithosphere and origin of K-rich volcanism in post-collisional settings. J. Volcanol. Geoth. Res., 198, 112-128, doi: 10.1016/j.jvolgeores.2010.08.014, 2010.
Feininger, T., Seguin, M.K.: Simple Bouguer gravity anomaly field and the inferred crustal structure of continental Ecuador. Geology, 11, 40-44, doi: 10.1130/0091-7613(1983)11<40:SBGAFA>2.0.CO;2, 1983.
Fontboté, L., Kouzmanov, K., Chiaradia, M., Pokrovski, G.S.: Sulfide minerals in hydrothermal deposits. Elements, 13, 97-103, doi: 10.2113/gselements.13.2.97, 2017.
Fulignati P., Gioncada, A., Costa, S., Di Genova, D., Di Traglia F., Pistolesi, M.,: Magmatic sulfide immiscibility at an active magmatic-hydrothermal system: The case of La Fossa (Vulcano, Italy). J. Volcanol. Geoth. Res., 358 45–57, doi: 10.1016/j.jvolgeores.2018.06.009, 2018.
Georgatou, A., Chiaradia, M., Rezeau, H., Walle, M.: Magmatic sulphides in Quaternary Ecuadorian arc magmas. Lithos, 296-299, 580–599, doi: 10.1016/j.lithos.2017.11.019, 2018.
Grutzner, T., Prelević, D., Cüneyt, A.: Geochemistry and origin of ultramafic enclaves and their basanitic host rock from Kula Volcano, Turkey. Lithos, 180-181, 58-73, doi: 10.1016/j.lithos.2013.08.001, 2013.
Guillier, B., Chatelain, J., Jaillard, E., Yepes, H., Poupinet, G., Fels, J.: Seismological evidence on the geometry of the orogenic system in central-northern Ecuador (South America). Geophys. Res. Lett., 28, 3749–3752, doi: 10.1029/2001GL013257, 2001.
Hall, D.J., Foster, R.P., Yildiz, B., Redwood, S.D.: The Inlice High-sulphidation Epithermal Gold Discovery: Defining a Potential New Gold Belt in Turkey. Digging Deeper, Proceedings of the Ninth Biennial Meeting of the Society for Geology Applied to Mineral Deposits (January) 113–116, 2007.
Halter, W.E., Heinrich, C.A., Pettke, T.: Magma evolution and the formation of porphyry Cu–Au ore fluids: evidence from silicate and sulfide melt inclusions. Miner. Deposita, 39, 845-863, doi: 10.1007/s00126-004-0457-5, 2005.

https://doi.org/10.5194/se-2019-106
Preprint. Discussion started: 26 July 2019
© Author(s) 2019. CC BY 4.0 License.

Hattori, K.: High-sulfur magma, a product of fluid discharge from underlying mafic magma: Evidence from Mount Pinatubo, Philippines. Geology, 21, 1083-1086, doi: 10.1130/0091-7613(1993)021<1083:HSMAPO>2.3.CO;2, 1993.

Hattori, K.: Occurrence and origin of sulfide and sulfate in the 1991 Mount Pinatubo eruption products. In: Newhall, C.G., Punongbayan, R.S. (Eds.), Fire and Mud: Eruptions and Lahars of Mount Pinatubo, Philippines. University of Washington Press, 807–824, USGS, https://pubs.usgs.gov/pinatubo/hattori/, 1996.

Holwell, D., McDonald, I.: A review of the behaviour of platinum group elements within natural magmatic sulfide ore systems. Platin. Me. Rev., 54, 26-36, doi: 10.1595/147106709X480913, 2010.

Holwell, D., Keays, R., McDonald, I., Williams, M.: Extreme enrichment of Se, Te, PGE and Au in Cu sulfide microdroplets: evidence from LA-ICP-MS analysis of sulfides in the Skaergaard Intrusion, east Greenland. Contrib. Mineral. Petr., 170, 53, doi: 10.1007/s00410-015-1203-y, 2015.

Hou, Z., Zhang, H., Pan, X., and Yang, Z.: Porphyry Cu (–Mo–Au) deposits related to melting of thickened mafic lower crust: examples from the eastern Tethyan metallogenic domain. Ore Geol. Rev., 39, 21-45, doi: 10.1016/j.oregeorev.2010.09.002, 2011.

Innocenti, F., Agostini, S., Di Vincenzo, G., Doglioni, C., Manetti, P., Savaşçin, M. Y., Tonarini, S.: Neogene and Quaternary volcanism in Western Anatolia: magma sources and geodynamic evolution. Mar. Geol., 221, 397-421, doi: 10.1016/j.margeo.2005.03.016, 2005.

Jenner, F.: Cumulate causes for the low contents of sulfide-loving elements in the continental crust. Nat. Geosci., 10, 524–529, doi: 10.1038/ngeo2965, 2017.

Jenner, F., O'Neill, H., Arculus, R., Mavrogenes, J.: The magnetite crisis in the evolution of arc-related magmas and the initial concentrations of Au, Ag, and Cu. J. Petrol., 2445–2464, doi: 10.1093/petrology/egq063, 2010.

Jensen, E.: Pyrrhotite: melting relations and composition: Am. J. Sci., 240, 695-709, doi: 10.2475/ajs.240.10.695, 1942.

Karaoğlu, Ö., Helvacı, C., Ersoy, Y.: Petrogenesis and 40 Ar/39 Ar geochronology of the volcanic rocks of the Uşak-Güre basin, western Türkiye. Lithos, 119, 193-210, doi: 10.1016/j.lithos.2010.07.001, 2010.

Keith, J.D., Whitney, J.A., Hattori, K., Ballantyne, G.H., Christiansen, E.H., Barr, D.L., Cannan, T.M. and Hook, C.J.: The role of magmatic sulfides and mafic alkaline magmas in the Bingham and Tintic mining districts, Utah. J. Petrol., 3 1679–1690, doi: 10.1093/petroj/38.12.1679, 1997.

Keith, M., Haase, K., Klemd, R., Schwarz-Schampera, U., Franke, H.: Systematic variations in magmatic sulphide chemistry from mid-ocean ridges, back-arc basins and island arcs. Chem. Geol., 451, 67-77, doi: 10.1016/j.chemgeo.2016.12.028, 2017.

Keller, J., Burgath K., Jung D., Wolff, F.: Geologie und petrologie des neogenen kalkalkali-vulkanismus von Konya (Erenler Dag-Alaca Dag-Massiv, Zentral-Anatolien) Geologisches Jahrbuch 25, 37-117, 1977.

Kelley, K.A., Cottrell, E.: Water and the oxidation state of subduction zone magmas. Science, 325, 605–607, doi: 10.1126/science.1174156, 2009.

Korkmaz, G., Kursad, A., Huseyin, K., Ganerod, M.: 40Ar/39Ar geochronology, elemental and Sr-Nd-Pb isotope geochemistry of the Neogene bimodal volcanism in the Yükselen area, NW Konya (Central Anatolia, Turkey). J. African Earth Sci., 129, 427-444, 2017.

Kullerud, G., Yund, R.A., Moh, G.H.: Phase relation in the Cu-Fe-Ni, Cu-Ni-S and Fe-Ni-S systems. Econ. Geol., 4, 323–343, doi: 10.1016/j.jafrearsci.2017.02.001, 1969.

Larocque, A.C., Stimac, J.A., Keith, J.D., Huminicki, M.A.: Evidence for open-system behavior in immiscible Fe–S–O liquids in silicate magmas: implications for contributions of metals and sulfur to ore-forming fluids. Can. Mineral., 38, 1233–1249, doi: 10.2113/gscanmin.38.5.1233, 2000.

Li, J., Qin, K.Z., Li, G.: Basic characteristics of gold-rich porphyry copper deposits and their ore sources and evolving processes of high oxidation magma and ore-forming fluid. Acta Petrol. Sin., 22, 678-688, 2006.

Loucks, R.B.: Distinctive composition of copper-ore-forming arc magmas. Aust. J. Earth Sci., 61, 5–16, doi: 10.1080/08120099.2013.865676, 2014.

Mandon, C.L.: Volatile transport of metals in the andesitic magmatic-hydrothermal system of White Island. M.S. thesis. Victoria University of Wellington, Hdl:10063/32. Web., 2017.

Metrich, N., Berry, A.J., O'Neill, H.S., Susini, J.: The oxidation state of sulfur in synthetic and natural glasses determined by X-ray absorption spectroscopy. Geochimica et Cosmochimica Acta 73, 2382-2399, doi: 10.1016/j.gca.2009.01.025, 2009.

Mungall, J., Brenan, J.: Partitioning of platinum-group elements and Au between sulfide liquid and basalt and the origins of mantle–crust fractionation of the chalcophile elements. Geochim. Cosmochim. Ac., 125, 265–289, doi: 10.1016/j.gca.2013.10.002, 2014.

Nadeau, O., Williams-Jones, A.E., Stix, J.: Sulphide magma as a source of metals in arc-related magmatic hydrothermal ore fluids. Nat. Geosci., 3, 501−505, doi: 10.1038/ngeo899, 2010.

Naldrett, A.: Magmatic Sulfide Deposits Geology, Geochemistry and Exploration. Springer Science and Business Media. Chapter 2: Theoretical considerations. doi: 10.1007/978-3-662-08444-1, 2013

Naldrett, A., Gasparrini E.: Archean nickel sulfide deposits in Canada: their classification geological setting and

https://doi.org/10.5194/se-2019-106
Preprint. Discussion started: 26 July 2019
© Author(s) 2019. CC BY 4.0 License.

genesis with some suggestions as to exploration. Geol. Soc. Aust. S., 3, 201-226, doi: 10.1007/978-3-662-08444-1. 1971.

Parat, F., Holtz, F., Streck, M.J.: Sulfur-bearing Magmatic Accessory Minerals. Rev. Mineral. Geochem., 73, 285-314, doi: 10.2138/rmg.2011.73.10, 2011.

Park, J.W., Campbell, I., Kim, J., Moon, J.-W.: The role of sulfide saturation on formation of a Cu- and Au-rich magma: insights from the platinum group element geochemistry of Niuatahi–Motutahi lavas, Tonga rear arc. J. Petrol., 56, 59–81, doi: 10.1093/petrology/egu071, 2015.

Patten, C., Barnes, S.J., Mathez, E.A.: Textural variations in MORB sulfide droplets due to differences in crystallization history. Can. Mineral., 50, 675–692, doi: 10.3749/canmin.50.3.675, 2012.

Pe-Piper, G., Piper, D.J.: Late Cenozoic, post-collisional Aegean igneous rocks: Nd, Pb and Sr isotopic constraints on petrogenetic and tectonic models. Geol. Magazine, 138, 653-668, doi: 10.1017/S0016756801005957, 2001.

Prelević, D., Akal, C., Foley, S.F., Romer, R.L., Stracke, A., Van Den Bogaard, P.: Ultrapotassic mafic rocks as geochemical proxies for post-collisional dynamics of orogenic lithospheric mantle: the case of southwestern Anatolia, Turkey. J. Petrol., 53, 1019-1055, doi: 10.1093/petrology/egs008, 2012.

Redwood, S.D.: Exploration of the Doğanbey Project, Konya, Turkey. Report for Stratex International plc, London, April, 26, 2006.

Richards, J.P.: Giant ore deposits form by optimal alignments and combinations of geological processes: Nat. Geosci., 6, 911–916, doi: 10.1038/ngeo1920, 2013.

Richards, J.: Postsubduction porphyry Cu-Au and epithermal Au deposits: Products of remelting of subduction-modified lithosphere. Geology, 37, 247–250, doi: 10.1130/G25451A.1, 2009.

Richards, J.: High Sr/Y arc magmas and porphyry Cu Mo Au deposits: Just add water. Econ. Geol., 106, 1075–1081, doi: 10.2113/econgeo.106.7.1075, 2011.

Richardson-Bunbury, J.M.: The Kula volcanic field, western Turkey; the development of a Holocene alkali basalt province and the adjacent normal-faulting graben. Geol. Magazine, 133, 275–283, doi: 10.1017/S0016756800009018, 1996.

Savelyev, D.P., Kamenetsky, V.S., Danyushevsky, L.V., Botcharnikov, R.E., Kamenetsky, M.B., Park, J.-W., Portnyagin, M.V., Olin, P., Krasheninnikov, S.P., Hauff, F.: Immiscible sulfide melts in primitive oceanic magmas: Evidence and implications from picrite lavas (Eastern Kamchatka, Russia). Am. Mineral., 103, 886–898, doi: 10.2138/am-2018-6352, 2018.

Schütte, P., Chiaradia, M., Barra, F., Villagómez, D., Beate, B.: Metallogenic features of Miocene porphyry Cu and porphyry-related mineral deposits in Ecuador revealed by Re–Os, 40Ar/39Ar, and U–Pb geochronology. Mineral. Deposita, 47, 383–410, doi: 10.1007/s00126-011-0378-z, 2012.

Seyitoglu, G.: Late Cenozoic tectono-sedimentary development of the Selendi and Usak-Güre basins: a contribution to the discussion on the development of east–west and north trending basins in western Turkey. Geol. Magazine, 134, 163-175, doi: 10.1017/S0016756897006705, 1997.

Shafiei, B., Haschke, M., Shahabpour, J.: Recycling of orogenic arc crust triggers porphyry Cu mineralisation in Kerman Cenozoic arc rocks, south-eastern Iran. Mineral. Deposita, 44, 265–283, doi: 10.1007/s00126-008-0216-0, 2009.

Sillitoe, R.: A Plate Tectonic Model for the Origin of Porphyry Copper Deposits. Econ. Geol., 67, 184-197, doi: 10.2113/gsecongeo.67.2.184, 1972.

Sillitoe, R.: Gold-rich porphyry copper deposits: Geological model and exploration implications. Geol. Associ. Can. S., 40, 465-478, https://eurekamag.com/research/019/092/019092917.php, 1993.

Sillitoe, R.: Some metallogenic features of gold and copper deposits related to alkaline rocks and consequences for exploration. Mineral. Deposita, 37, 4–13, doi: 10.1007/s00126-001-0227-6, 2002.

Sillitoe, R.: Copper provinces, in Hedenquist, J.W., et al., eds., Geology and Genesis of Major Copper Deposits and Districts of the World: A Tribute to Richard H. Sillitoe: Soc. Eco. Geo. Spc. Pub., 16, 1–18, doi: 10.5382/SP.17, 2012.

Temel, A.: Post-collisional Miocene alkaline volcanism in the oglakçi region, Turkey: Petrol. Geochem. Int. Geol. Rev., 43, 640–660, doi: 10.1080/00206810109465038, 2001.

Temel, A., Gundogdu, M.N., Gourgaud, A.: Petrological and geochemical characteristics of Cenozoic high-K calc-alkaline volcanism in Konya, Central Anatolia, Turkey. J. Volcanol. Geoth. Res., 85, 327–354, doi: 10.1016/S0377-0273(98)00062-6, 1998.

Tokçaer, M., Agostini, S., Savaşçın, M.Y.: Geotectonic setting and origin of the youngest Kula volcanics (western Anatolia), with a new emplacement model. Turk. J., Earth Sci., 14, 145–166, 2005.

Tsujimura T., Kitakaze, A.: New phase relations in the Cu–Fe–S system at 800°C; constraint of fractional crystallization of a sulfide liquid. Neues Jahrbuch für Mineralogie - Monatshefte, 10, 433-444, doi: 10.1127/0028-3649/2004/2004-0433, 2004.

Westaway, R., Pringle, M., Yurtmen, S., Demir, T., Bridgland, D., Rowbotham, G., Maddy, D.: Pliocene and Quaternary regional uplift in western Turkey: the Gediz River terrace staircase and the volcanism at Kula. Tectonophysics, 391, 121–169, doi: 10.1016/j.tecto.2004.07.013, 2004.

https://doi.org/10.5194/se-2019-106
Preprint. Discussion started: 26 July 2019
© Author(s) 2019. CC BY 4.0 License.

Wilke, M., Klimm, K., Kohn, S.C.: Spectroscopic Studies on Sulfur Speciation in Synthetic and Natural Glasses. Rev. Mineral. Geochem., 73, 41-78, doi: 10.2138/rmg.2011.73.3, 2011.

Wilkinson, J.J.: Triggers for the formation of porphyry ore deposits in magmatic arcs. Nat. Geosci., 6, 917–925, doi: 10.1038/ngeo1940, 2013.

Yang, Z.M., Lu, Y.J., Hou, Z.Q., Chang, Z.S.: High-Mg diorite from Qulong in southern Tibet: Implications for the genesis of adakite-like intrusions and associated porphyry Cu deposits in collisional orogens. J. Petrol., 56, 227–254, doi: 10.1093/petrology/egu076, 2015.

Yund, R., Kullerud, G.: Thermal stability of assemblages in Cu-Fe-S system. J. Petrol., 7, 456-488, doi: 10.1093/petrology/7.3.454, 1966.

Zelenski, M., Kamenetsky, V.S., Mavrogenes, J.A., Gurekno, A.A., Danyushevsky, L.V.: Silicate– sulfide liquid immiscibility in modern arc basalt (Tolbachik volcano, Kamchatka): part I. Occurrence and compositions of sulfide melts. Chem. Geol., 471, 92–110, doi: 10.1016/j.chemgeo.2017.09.019, 2017.

Zhang, D., Audétat A.: Chemistry, mineralogy and crystallization conditions of porphyry Mo-forming magmas at Urad-Henderson and silver creek, Colorado, USA. J. Petrol., 58, 277-296, doi: 10.1093/petrology/egx016, 2017.

Zürcher, L., Bookstrom, A.A., Hammarstrom, J.M., Mars, J.C., Ludington, S., Zientek, M.L., Dunlap, P., Wallis, J.C., with contributions from Drew, L.J., Sutphin, D.M., Berger, B.R., Herrington, R.J., Billa, M., Kuşcu, I., Moon, C.J., Richards, J.P.: Porphyry copper assessment of the Tethys region of western and southern Asia: U.S. Geol. Surv. Sci. Invest. Rep., 2010-5090, 232, and spatial data, doi:10.3133/sir20105090V, 2015.

https://doi.org/10.5194/se-2019-106
Preprint. Discussion started: 26 July 2019
© Author(s) 2019. CC BY 4.0 License.

Solid Earth
Discussions
Open Access
EGU

Tables and Table Captions

Table 1. EPMA summary for individual sulphide analysis (N=number of measurements) corresponding to each sulphide type for every study area. The empty cells (-) correspond to a lack of measurement either because it was ~~under~~ determination limit or ~~because it was~~ not measured~~,~~ for complete dataset, analytical conditions and detection limits see Table 4 in doi:10.6084/m9.figshare.8230787.

Area	Type (N)		Whole Rock Chemistry		EPMA Sulphide Chemistry (wt %)									
			Cu ppm	SiO2 wt%	S	Cu	Fe	Ni	As	Se	Zn	Ag	Au	Tot
Beydagi	2 (17)	med	7	62	38	0.3	55	0.15	0.03	0.2	0.5	0.02	0.22	98
		min	4.2	46	35	0.01	29	0.03	0.03	0.02	0.5	0.01	0.15	-
		max	29	72	53	34	58	0.77	0.03	0.02	0.5	0.02	0.27	-
		av	12	62	40	6.6	49	0.31	0.03	0.02	0.5	0.02	0.22	99
		SD	6.7	3.9	5.7	11	10	0.28	-	-	-	-	0.05	-
	3 (16)	med	18	59	35	32	31	0.12	0.07	0.03	0.98	0.01	0.24	99
		min	6.7	59	33	0.17	31	0.01	0.07	0.03	0.73	0.01	0.24	-
		max	18	63	53	33	58	1.21	0.07	0.03	3	0.02	0.24	-
		av	17	59	38	24	35	0.32	0.07	0.03	1.4	0.01	0.24	99
		SD	2.8	1	6.1	13	7.6	0.43	-	-	0.9	-	-	-
	5 (6)	med	6.7	63	38	0.78	56	0.04	-	-	0.71	0.02	0.14	97
		min	6.7	59	33	0.08	29	0.01	-	-	0.59	0.02	0.14	-
		max	18	63	51	32	58	0.21	-	-	2.4	0.02	0.14	-
		av	10	61	38	11	47	0.07	-	-	1.2	0.02	0.14	97
		SD	5.6	2.1	5.3	15	13	0.07	-	-	1.03	-	-	-
Itecektepe	2 (26)	med	7	62	38	0.03	57	0.1	-	0.04	0.81	0.02	0.18	97
		min	5.1	61	35	0.01	52	0.02	-	0.04	0.57	0.01	0.18	-
		max	13	64	39	6.1	58	0.25	-	0.04	1.5	0.03	0.18	-
		av	7.2	62	38	0.27	57	0.1	-	0.04	0.88	0.02	0.18	97
		SD	1.6	0.85	0.85	1.2	1.3	0.05	-	-	0.34	0.01	-	-
Elmadag	2 (8)	med	26	61	37	0.14	56	0.26	0.04	-	0.75	0.02	-	96
		min	4.3	56	35	0.01	32	0.04	0.04	-	0.72	0.02	-	-
		max	63	69	39	29	58	1.5	0.04	-	0.79	0.02	-	-
		av	26	61	37	4.2	53	0.4	0.04	-	0.75	0.02	-	96
		SD	12	2.9	1.29	11	8.73	0.47	-	-	0.05	-	-	-
Kula	1 (10)	med	29	47	38	0.05	56	4.2	0.04	0.02	-		0.04	98
		min	29	47	36	0.03	45	3	0.03	0.02	-	-	0.04	-
		max	30	48	39	0.34	57	14	0.06	0.03	-	-	0.04	-
		av	29	48	38	0.15	54	6	0.04	0.02	-	-	0.04	98
		SD	0.25	0.35	0.76	0.14	4.4	4.3	0.01	-	-	-	-	-
	2 (190)	med	29	47	38	0.1	58	0.77	0.04	0.04	0.03	0.02	0.05	98
		min	23	37	38	0.01	5.8	0.01	0.02	0.02	0.02	0.01	0.03	-
		max	61	66	40	32	62	41	0.1	0.08	0.16	0.04	0.22	-
		av	30	47	36	2.4	54	2.9	0.05	0.04	0.05	0.02	0.06	98
		SD	4.2	1.7	5.9	6.3	10	7.3	0.02	0.01	0.04	0.01	0.04	-
	5 (35)	med	29	47	37	0.45	59	0.78	0.05	0.03	0.03	0.02	0.04	98
		min	28	47	33	0.01	35	0.04	0.02	0.02	0.02	0.01	0.03	-
		max	35	48	40	26	61	22	0.08	0.06	0.16	0.05	0.11	-

https://doi.org/10.5194/se-2019-106
Preprint. Discussion started: 26 July 2019
© Author(s) 2019. CC BY 4.0 License.

		av	30	47	37	4.7	55	1.8	0.05	0.04	0.05	0.02	0.05	98
		SD	2.6	0.31	1.8	8.5	8.3	4.1	0.01	0.01	0.04	0.01	0.02	-
		med	12	61	38	0.09	58	0.11	0.04	0.02	0.04	0.05	-	97
		min	4.6	46	26	0.01	15	0.01	0.02	0.01	0.01	0.01	-	-
	2 (187)	max	50	70	48	69	60	9.4	0.08	0.05	0.23	0.11	-	-
		av	13	62	37	4.2	55	0.23	0.04	0.02	0.04	0.05	-	96
Konya		SD	4.8	2.9	3.2	11	8.7	0.79	0.02	0.01	0.04	0.03	-	-
		med	13	62	26	56	16	0.01	0.05	0.02	0.06	0.06	-	99
		min	12	61	22	38	5.6	0.01	0.02	0.02	0.06	0.04	-	-
	4 (19)	max	21	62	33	72	29	0.11	0.06	0.02	0.06	0.07	-	-
		av	14	62	27	54	18	0.02	0.04	0.02	0.06	0.06	-	99
		SD	3.5	0.33	3.1	11	7.1	0.02	0.02	-	-	0.01	-	-
		med	23	62	39	1.27	58	0.4	0.04	-	0.02	-	-	98
		min	6	48	20	0.01	17	0.01	0.01	-	0.02	-	-	-
	2 (172)	max	105	77	53	36	65	10	45	-	0.02	-	-	-
		av	27	62	38	11	52	0.68	1.18	-	0.02	-	-	98
Ecuador		SD	15	3.3	3.2	14	11	1.14	7.01	-	-	-	-	-
		med	32	60	27	56	17	0.39	0.08	-	-	0.02	-	100
		min	16	58	25	40	14	0.23	0.01	-	-	0.01	-	-
	4 (22)	max	38	64	32	66	27	0.56	0.32	-	-	0.02	-	-
		av	31	60	27	55	18	0.39	0.08	-	-	0.02	-	100
		SD	4.8	1.8	1.9	7.4	4.1	0.23	0.08	-	-	-	-	-

Table 2. Summary composition of 100 reconstructed sulphides belonging to different sulphide types (N=number of sulphides reconstructed) observed in every study area except Itecektepe and Elmadag ~~were~~ the Cu-rich phase was too small to analyse with the EPMA. The empty cells (-) correspond to a lack of measurement either because it was ~~under~~ determination limit or ~~because it was~~ not measured, for complete dataset (including mss/iss area% of Itecektepe and Elmadag) see Table 5 in doi:10.6084/m9.figshare.8230787.

		Whole Rock med		Area med%			EPMA med wt% Reconstruction									
Area	Type (N)	Cu ppm	SiO_2	mss	iss	void	S	Cu	Fe	Ni	As	Se	Zn	Ag	Au	Tot
Beydagi	2(1)	17.85	58.67	95.5	4.5	16.7	38.77	0.69	56.67	0.73	-	-	-	-	0.08	97
	3(8)	17.85	58.67	34.5	65.5	2.8	39.53	23.02	34.24	0.05	0.02	0.11	-	0.02	0.09	97
Kula	1 (4)	28.8	47.42	99.5	0.5	0	37.84	0.1	55.35	4.42	0.05	-	-	-	0.03	99
	2(25)	28.8	47.42	88.7	11.2	0.7	37.93	2.57	56.66	0.73	0.04	-	0.02	0.02	0.03	99
	5(8)	29	47.64	86.8	13.1	-	36.03	3.46	57.3	1.03	0.04	0.02	0.02	0.01	-	98
Konya	2(26)	11.71	61.27	89.5	10.8	0.4	38.66	2.73	56.78	0.11	0.03	0.03	0.03	0.03	0.02	98
	4(8)	12.68	61.82	0	100	21.2	28.31	48.44	23.09	0.02	0.02	0.02	0.04	0.04	-	99
Ecuador	2(10)	19	62.27	78.5	21.5	16.9	37.7	6.04	53.47	1.71	0.02	-	-	-	-	98
	4(10)	32	59.66	0	100	5.65	28.09	51.71	21.05	0.37	0.11	-	-	-	-	100

https://doi.org/10.5194/se-2019-106
Preprint. Discussion started: 26 July 2019
© Author(s) 2019. CC BY 4.0 License.

Solid Earth
Discussions
Open Access
EGU

Figure Captions

Figure 1. World distribution arc-related metallogenic belts showing the biggest Cu and/or Au porphyry deposits, modified from Richards, 2013 and Cooke et al., 2005. References of previous studies on magmatic sulphides are depicted with black stars whereas the areas considered in this study are shown with a red bigger star.

Figure 2. Tectonic (a) and geological maps (b-c) of the studied areas and associated Au epithermal and Cu, Au porphyry deposits in Western Anatolia. The investigated Miocene volcano-plutonic complexes are Konya (b) and the volcanoes of Usak basin (Elmadag, Itecektepe and Beydagi-c) as well as the Quaternary Kula volcano (c). The geological maps have been modified after; (b) Keller et al., 1977 and (c) Karaoglou et al., 2010.

Figure 3. Major (a-d) and trace (e-h) element variations with SiO_2 for the different study areas, illustrated by a different shape and colour. Smaller in size symbols correspond to datasets obtained from other studies (Beydagi-Karaoglou, 2010, Kula-Alici et al., 2002, Aldanmaz et al., 2002, 2015, Dilek et al., 2010, Ercan et al., 1985, Konya-Temel et al., 1998, Korkmaz et al., 2017). For comparison purposes whole rock chemistry from Ecuador has been illustrated as a field in the graphs (a-f). Spider graph-g showing the solid mean trace element distribution for the different study areas. For dataset see Tables 1-3 in doi:10.6084/m9.figshare.8230787

Figure 4. Sulphide types observed in the different study areas. ~~Note that only Konya and Ecuador present type-4 and only Beydagi shows type-3, sulphides.~~ The abbreviations stand for: pyrrhotite-po, pentlandite-pn, chalcopyrite-cp, chalcocite-cc, cubanite-cb, pyrite-py, bornite-bn, digenite-dg, anhydrite-anhy, apatite-apt, magnetite-mt monosulphide solid solution-mss and intermediate solid solution-iss. The scale bar corresponds to 5 μm unless stated otherwise.

Figure 5. BSE (a-f,h) and SEI (g) microphotographs of sulphides, their host and accessory mineral phases. Important things to note: a) the common occurrence of apatite inclusions observed together with the sulphide and hosted by the same mineral (px in a and mt in b,f); b) the lack of sulphides in the biotite phenocrysts, even in the cases where the biotite itself includes a magnetite that hosts sulphides; c) the usual sulphide presence in the amphibole destabilised rim, where amphibole is being replaced by clinopyroxene, plagioclase and rhönite, characterising the Kula volcano (also seen by Grutzner et al., 2013); d) resorbed sulphide found in amphibole in (c) showing a rapid unmixing of the cp-cb (iss); e) unusually big (up tp 600 μm) sulphide aggregate composed of mostly Cu-poor sulphides, magnetite and micro-sized silicates, found in Kula; f) partly dissolved sulphide hosted by magnetite that shows ilmenite exsolution lamellae, g) trail of bubbles of silicate melt and voids associated with the sulphide and h) daughter sulphide (<0.5 μm), composed mostly po found in re-crystallised melt inclusion hosted by olivine, observed in Kula. The scale bar corresponds to 100 μm unless stated otherwise.

Figure 6. BSE (a,b-i,c-i,e,f) and SEI (b-ii,c-ii,d,e) microphotographs of anhydrite occurrences in magnetite phenocrysts, as individual phases or found together with Cu-rich sulphides and occasionally with zircons. Apatite and silicate melt are often hosted by the same magnetite phenocrysts as well. Note that the anhydrite; (b-i,f) in BSE is not visible unless seen in SEI (b-ii), it can be partly (d,e) or completely (c) dissolved. In image-e BSE and

https://doi.org/10.5194/se-2019-106
Preprint. Discussion started: 26 July 2019
© Author(s) 2019. CC BY 4.0 License.

SEI imagining have been merged in order to make both sulphide and sulphate, respectively visible. The scale bar corresponds to 2 μm unless stated otherwise.

Figure 7. Sulphide composition in the Cu-Fe-S system and Ni-Fe-Cu from individual analyses by EPMA. The colour shows the study area and the shape indicates the host mineral in which magmatic sulphides were found. Note the progressive Ni/Cu depletion as we switch from more mafic suites (e.g. Kula) and early crystallising host minerals (olivine, pyroxene and amphibole) to more evolved (e.g. Konya) and later crystallising mineral phases (magnetite). The grey fields correspond to analysis that resulted in Ni or Cu below determination limit equal to 0.01 wt% that however for discussion purposes have been shown here. The measurements depicted with an error bar (cross) represent SEM analysis where the mineral phase was too small to analyse by EPMA, the error does not correspond to a quantitative value. For dataset see Table 4 in doi:10.6084/m9.figshare.8230787.

Figure 8. Box plot comparison of the Cu and Ni content (wt %) measured by EPMA for the different sulphide types characterising each study area. The central box is in the middle 50% of the data (total number of measurements considered is noted in parenthesis on the x axes). The line and dots in the box represent the median and mean value for each box/sulphide type, respectively (see values in table 1). The outliers are further than 1.5*(75th percentile/top of box-25th percentile/bottom of box) and the whiskers are the extreme values that are not outliers. Note that only Beydagi, Konya and Ecuador which are the three areas associated with porphyry deposits display the highest in Cu values of type 3 and 4 sulphides. For dataset see Table 4 in doi:10.6084/m9.figshare.8230787.

Figure 9. Box plot comparison of the Cu-rich phase (cp = iss) and Ni-rich phase (po±pn = mss) proportions (area %) composing type-2 sulphides, calculated by ImageJ©1.38 software analysis for each study area (N of sample; Kula=25, Itecektepe=16, Elmadag=10, Beydagi=15, Konya=25, Ecuador=35). Average, mean and median values are represented in the graph same as in figure 8. For dataset see Table 5 in doi:10.6084/m9.figshare.8230787.

Figure 10. Ternary isothermal sections through the central part of the Cu-Fe-S system according to and modified from (a,b,c) Kullerud et al., 1969, (d) Tsujimura and Kitakaze, 2004, (e) Cabri, 1973, (f,h) Yund and Kullerud 1966, (g) Craig and Scot, 1974. The stability fields and phase-relations at different temperatures are shown for; sulphide liquid-L (brown), bornite solid solution-bnss (purple), monosulphide solid solution-mss (pink), intermediate solid solution-iss (yellow) and digenite solid solution-dgss (blue). The data shown correspond to the bulk (area %) reconstructed sulphide compositions hosted by different phenocrysts/groundmass (shape) observed in every study areas (colour). For dataset see Table 5 in doi:10.6084/m9.figshare.8230787.

https://doi.org/10.5194/se-2019-106
Preprint. Discussion started: 26 July 2019
© Author(s) 2019. CC BY 4.0 License.

Solid Earth
Discussions
Open Access
EGU

Figures

Fig.1

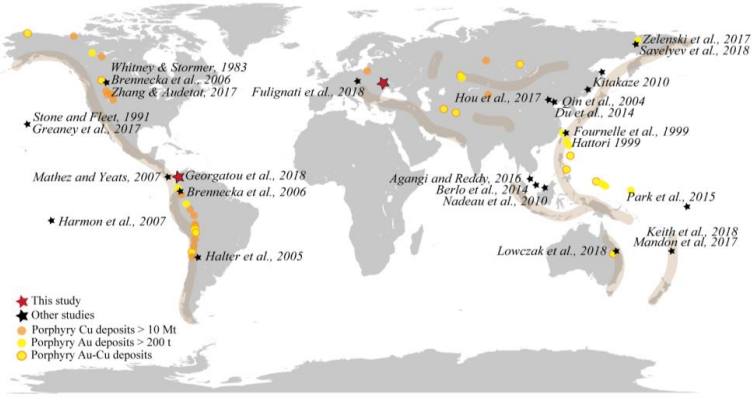

https://doi.org/10.5194/se-2019-106
Preprint. Discussion started: 26 July 2019
© Author(s) 2019. CC BY 4.0 License.

Solid Earth
Discussions
Open Access
EGU

Fig.2

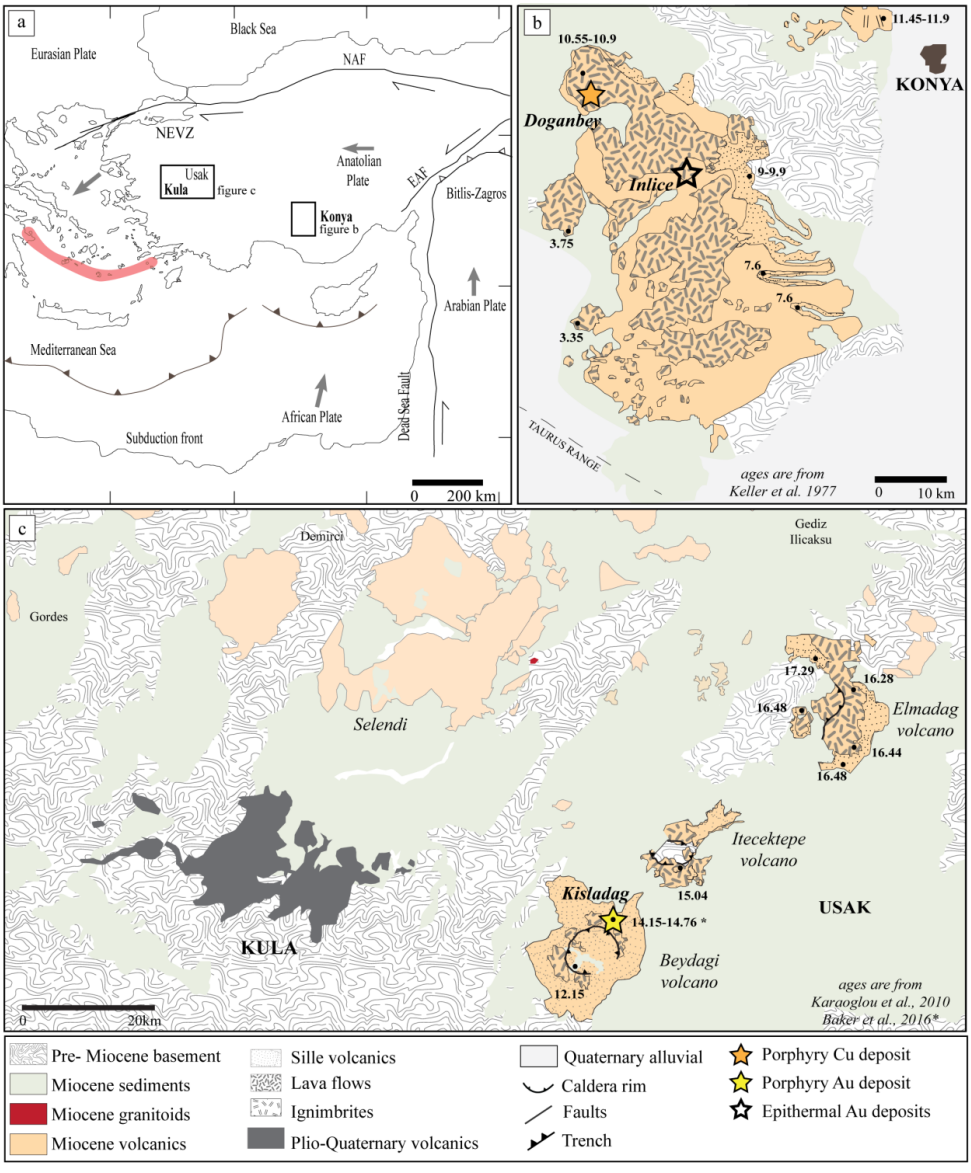

820

https://doi.org/10.5194/se-2019-106
Preprint. Discussion started: 26 July 2019
© Author(s) 2019. CC BY 4.0 License.

Solid Earth
Discussions
Open Access
EGU

Fig.3

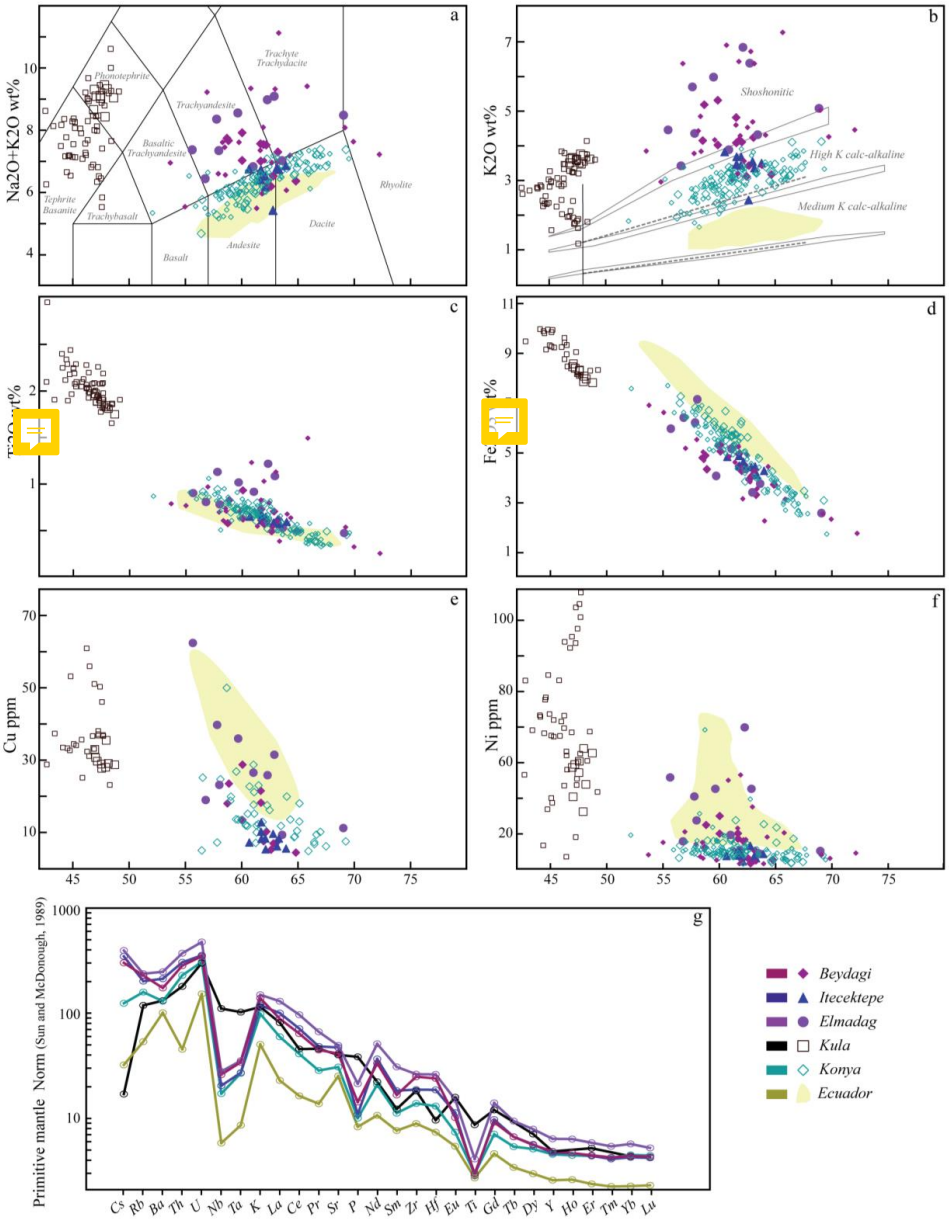

https://doi.org/10.5194/se-2019-106
Preprint. Discussion started: 26 July 2019
© Author(s) 2019. CC BY 4.0 License.

824 **Fig.4**

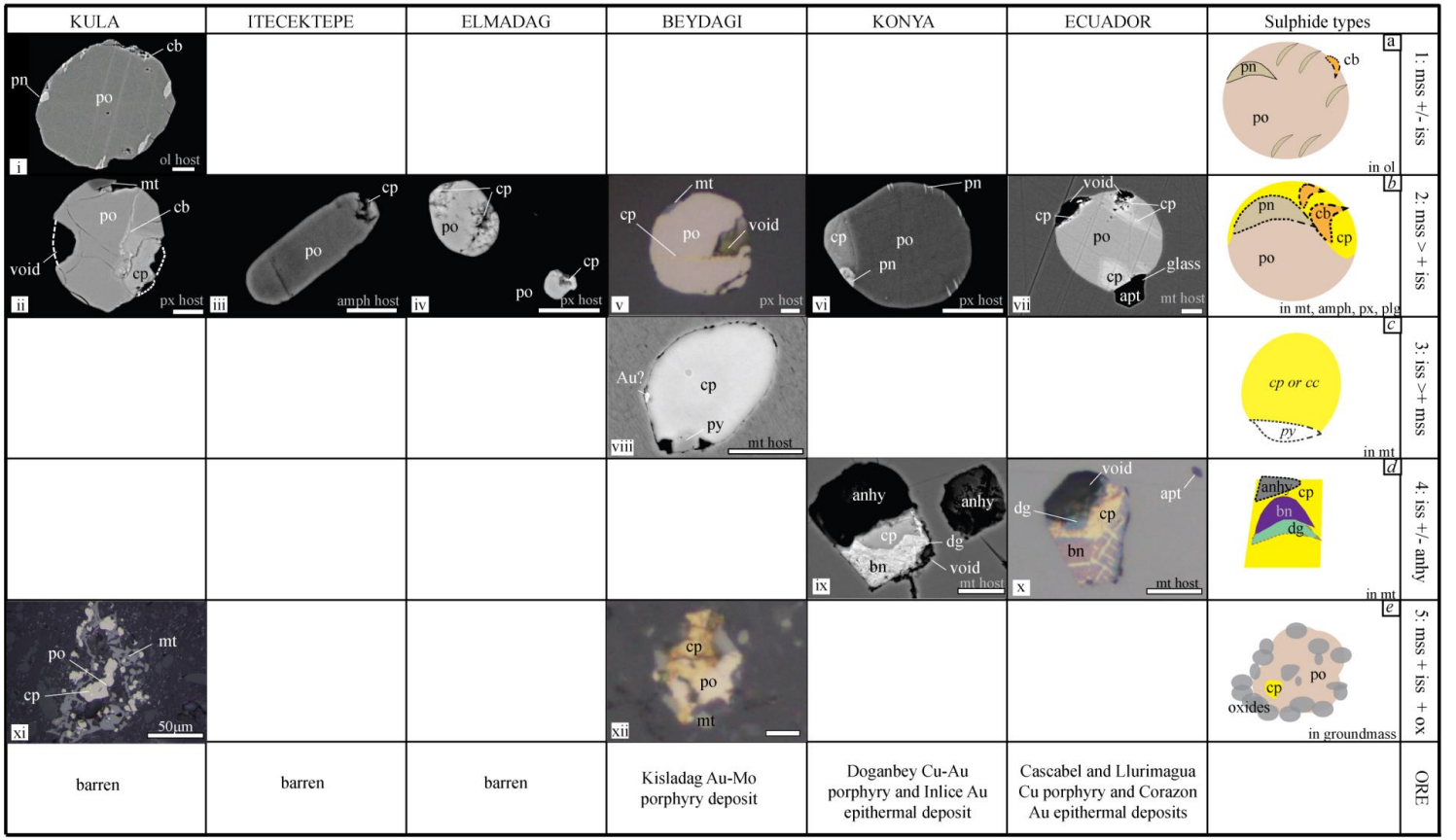

825

https://doi.org/10.5194/se-2019-106
Preprint. Discussion started: 26 July 2019
© Author(s) 2019. CC BY 4.0 License.

Solid Earth
Discussions
Open Access
EGU

826 **Fig.5**

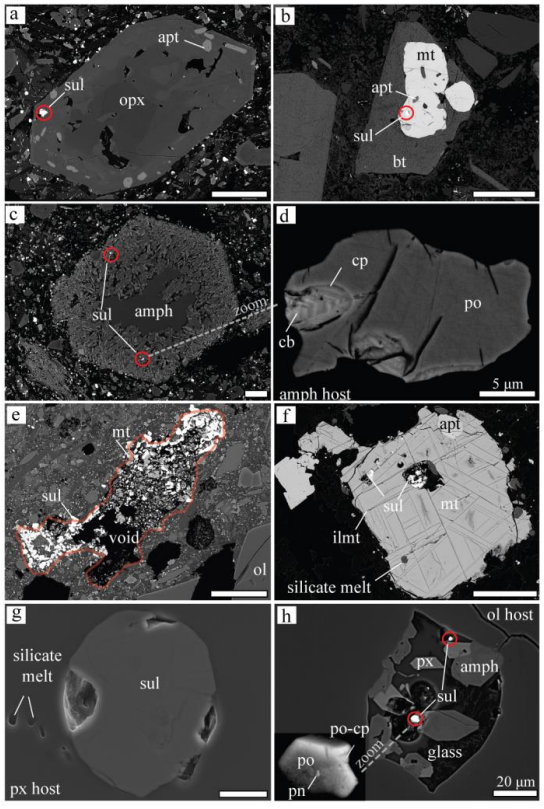

827

828 **Fig.6**

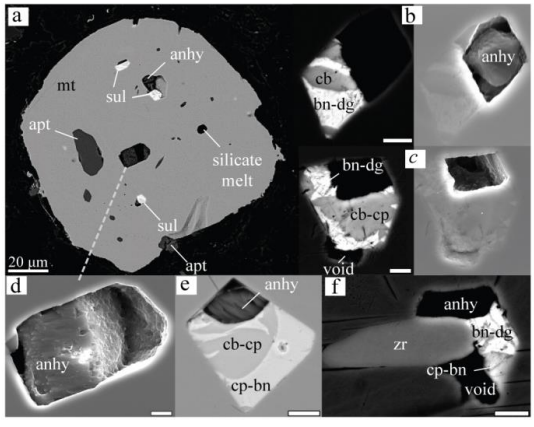

829

830

https://doi.org/10.5194/se-2019-106
Preprint. Discussion started: 26 July 2019
© Author(s) 2019. CC BY 4.0 License.

831 **Fig.7**

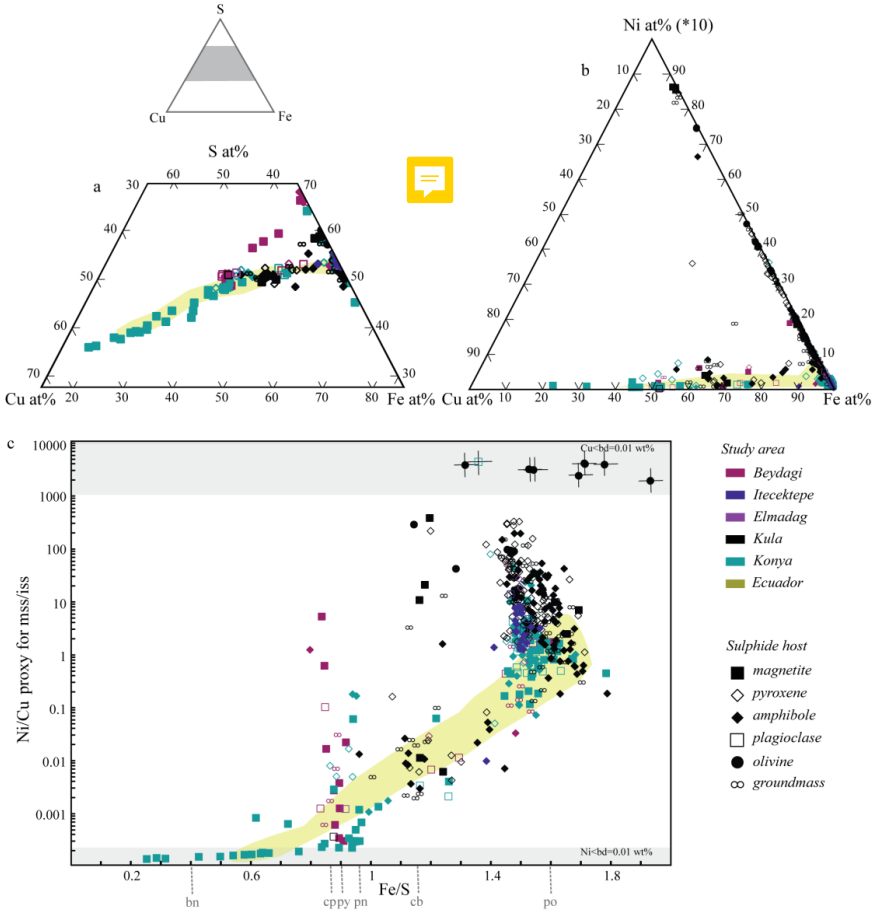

832

https://doi.org/10.5194/se-2019-106
Preprint. Discussion started: 26 July 2019
© Author(s) 2019. CC BY 4.0 License.

833 **Fig.8**

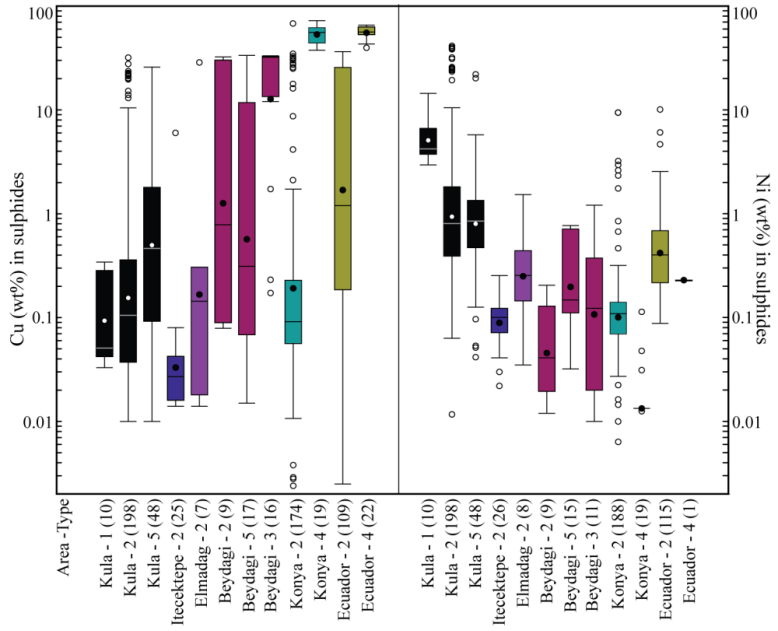

834

835 **Fig.9**

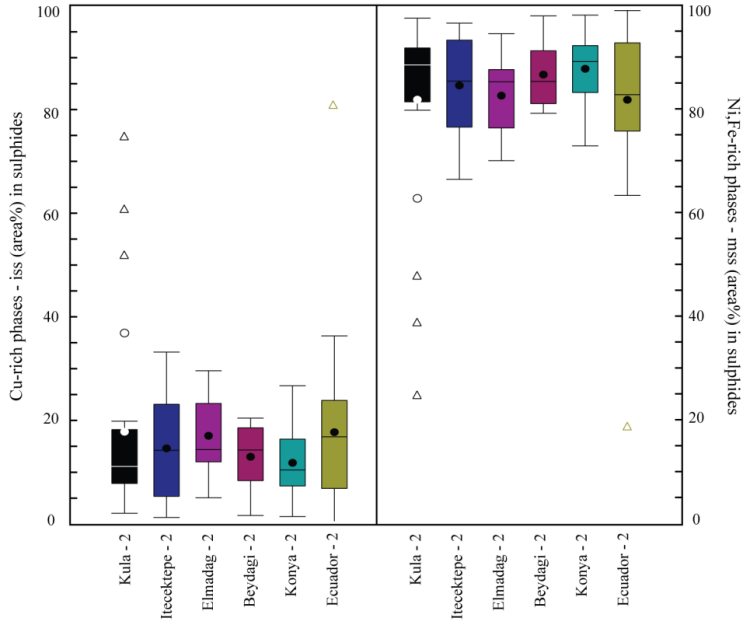

836

https://doi.org/10.5194/se-2019-106
Preprint. Discussion started: 26 July 2019
© Author(s) 2019. CC BY 4.0 License.

Solid Earth
Discussions
Open Access
EGU

837 **Fig.10**

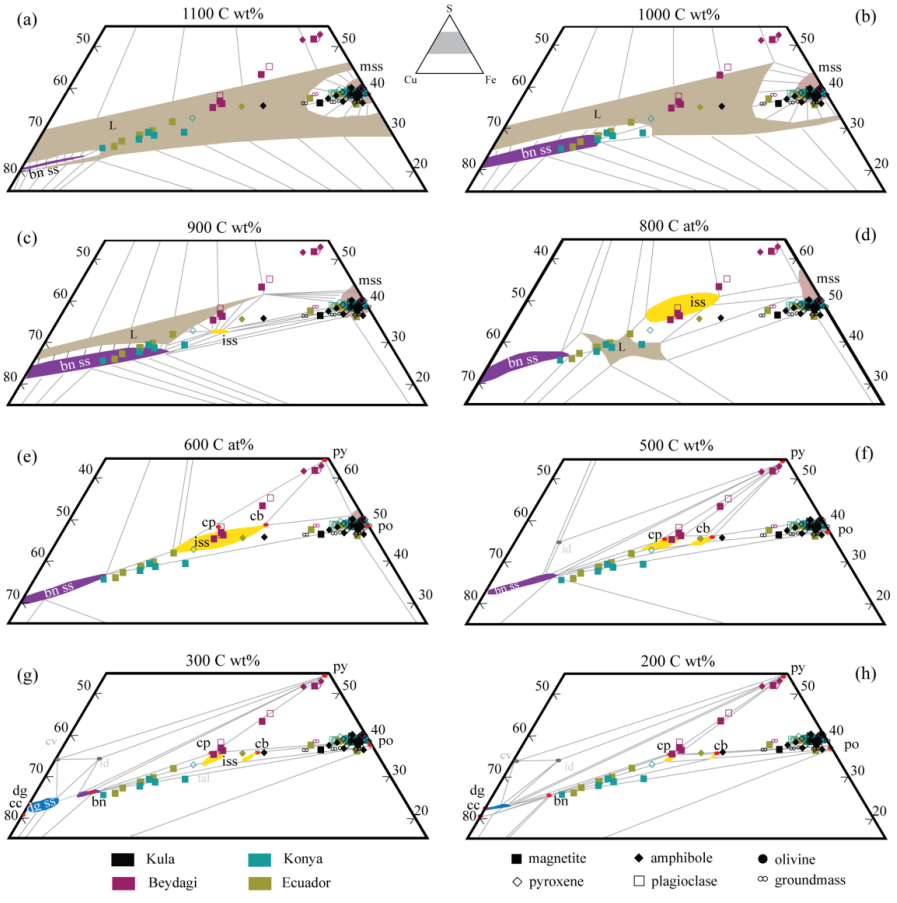

838